Inducible deletion of skeletal muscle AMPKα reveals that AMPK is required for nucleotide balance but dispensable for muscle glucose uptake and fat oxidation during exercise.

Janne R. Hingst[1#], Rasmus Kjøbsted[1#], Jesper B. Birk[1], Nicolas O. Jørgensen[1], Magnus R. Larsen[1], Kohei Kido[1], Jeppe Kjærgaard Larsen[1], Sasha A. S. Kjeldsen[1], Joachim Fentz[1], Christian Frøsig[1], Stephanie Holm[1], Andreas M. Fritzen[1], Tine L. Dohlmann[2], Steen Larsen[2, 3], Marc Foretz[4], Benoit Viollet[4], Peter Schjerling[5], Peter Overby[6], Jens F. Halling[6], Henriette Pilegaard[6], Ylva Helsten[7] and Jørgen F. P. Wojtaszewski[1*]

[#] J. R. Hingst and R. Kjøbsted contributed equally to this study.

[1] Section of Molecular Physiology, Department of Nutrition, Exercise and Sports, Faculty of Science, University of Copenhagen, DK-2100 Copenhagen, Denmark.

[2] Section of Systems Biology Research, Department of Biomedical Sciences, Faculty of Health, University of Copenhagen, Denmark.

[3] Clinical Research Centre, Medical University of Bialystok, Bialystok, Poland.

[4] Université de Paris, Institut Cochin, CNRS UMR8104, INSERM, U1016, F-75014, Paris, France.

[5] Institute of Sports Medicine Copenhagen, Department of Orthopedic Surgery M, Bispebjerg Hospital and Center for Healthy Aging, Faculty of Health and Medical Sciences, University of Copenhagen, Denmark.

[6] Section for Cell Biology and Physiology, Department of Biology, University of Copenhagen, Denmark.

[7] Section of Integrative Physiology, Department of Nutrition, Exercise and Sports, Faculty of Science, University of Copenhagen, DK-2100 Copenhagen, Denmark.

[1] To whom correspondence should be addressed. Universitetsparken 13, 2100 Copenhagen, Denmark. Email: jwojtaszewski@nexs.ku.dk, phone: +45 35 32 16 25

Highlights:

- Inducible deletion of AMPKα in adult mice disturbs nucleotide balance during exercise, lowers muscle glycogen content and reduces exercise capacity.
- Muscle mitochondrial respiration, glucose uptake and FA oxidation during muscle contractile activity remains unaffected by muscle-specific deletion of AMPKα subunits in adult mice.

Abstract

Objective: Current evidence for AMPK-mediated regulation of skeletal muscle metabolism during exercise is mainly based on transgenic mouse models with chronic (lifelong) disruption of AMPK function. Findings based on such models are potentially biased by secondary effects related to chronic lack of AMPK function. In an attempt to study the direct effect(s) of AMPK on muscle metabolism during exercise, we generated a new mouse model with inducible muscle-specific deletion of AMPKα catalytic subunits in adult mice.

Methods: Tamoxifen-inducible and muscle-specific AMPKα1/α2 double KO mice (AMPKα imdKO) were generated using the Cre/loxP system with the Cre driven by the human skeletal muscle actin (HSA) promotor.

Results: During treadmill running at the same relative exercise intensity, AMPKα imdKO mice showed greater depletion of muscle ATP, which was associated with accumulation of the deamination product IMP. Muscle-specific deletion of AMPKα in adult mice promptly reduced maximal running speed, muscle glycogen content and was associated with reduced expression of UGP2, a key component of the glycogen synthesis pathway. Muscle mitochondrial respiration, whole body substrate utilization as well as muscle glucose uptake and fatty acid (FA) oxidation during muscle contractile activity remained unaffected by muscle-specific deletion AMPKα subunits in adult mice.

Conclusions: Inducible deletion of AMPKα subunits in adult mice reveals that AMPK is required for maintaining muscle ATP levels and nucleotide balance during exercise, but is dispensable for regulating muscle glucose uptake, FA oxidation and substrate utilization during exercise.

Keywords: AMPK, exercise, glucose uptake, muscle metabolism, fat oxidation, glycogen.

1. INTRODUCTION

Physical activity is associated with a marked increase in muscle metabolism and energy turnover [1]. Therefore, maintaining intracellular levels of adenosine triphosphate (ATP) during exercise represents a major metabolic challenge for the muscle cell. The increased ATP turnover during exercise leads to accumulation of intramyocellular adenosine monophosphate (AMP) in an exercise intensity- and duration-dependent manner due to the adenylate kinase reaction (2ADP ↔ ATP + AMP) [2]. The increased intramyocellular AMP/ATP ratio leads to activation of 5'-AMP-activated protein kinase (AMPK) [3], which promotes catabolic processes and inhibits anabolic processes in order to normalize the cellular energy status [4]. On this basis, skeletal muscle AMPK is proposed to function as a cellular energy sensor that is activated during exercise and thus acts as a central mediator of cellular signaling to maintain energy homeostasis.

Given its pivotal role in the regulation of muscle metabolism, AMPK activation provides a putative therapeutic target for metabolic disorders such as type 2 diabetes (T2D) [5]. Acute pharmacological activation of AMPK in rodent muscle by different pharmacological agents (e.g. AICAR, PF739 and MK-8722) promotes glucose disposal and fatty acid (FA) oxidation [6–8]. Yet, AMPK-deficient mouse models have provided conflicting results as to whether AMPK activation is required for muscle metabolism to cope with the cellular energy stress during exercise. While reduced muscle glucose uptake has been reported in AMPK deficient mice during *in vivo* treadmill exercise and contraction of isolated mouse muscles in some studies [9–15], other studies have demonstrated intact muscle glucose uptake during contractile activity [16–22]. Knockout (KO) of the two regulatory AMPKβ subunits (AMPKβ1β2M-KO) is associated with impaired muscle glucose uptake and increased FA oxidation during treadmill exercise [9], while KO of both catalytic AMPKα subunits

(AMPKα1/α2) in muscle (AMPKα mdKO mice) or KO of the AMPK upstream kinase liver kinase B1 (LKB1) (LKB1 KO mice) leads to increased reliance on glucose as a substrate during treadmill exercise [16,17]. However, direct interpretation of these findings is confounded by disrupted mitochondrial capacity [9,17] and changes in expression of key proteins/enzymes involved in lipid metabolism (e.g. CD36 and FABPpm) in these models [16,17].

In most studies, maximal treadmill running speed is reduced in AMPK deficient mice compared to wild type (control) littermates (see [23] for detailed review). During high metabolic stress, the muscle cell prevents accumulation of AMP by converting it to inosine monophosphate (IMP) in a AMP-deaminase (AMPD) dependent reaction that serves to maintain a homeostatic ATP/ADP ratio [24]. Accelerated ATP degradation and reduced glucose uptake has been observed in muscle from mice overexpressing a kinase-dead AMPKα2 construct (AMPKα2 KD mice) [10]. Whether these findings can be ascribed directly to the lack of functional AMPK or rather should be seen as a consequence of the marked impairment in mitochondrial function reported for this model remains unclear [10].

Taken together, previous findings in AMPK deficient mouse models indicate that the observed phenotypes may be ascribed to secondary effects due to the lifelong lack of AMPK rather than acute regulation of AMPK activity during e.g. exercise. In attempt to study the direct effect(s) of AMPK activation during exercise, we developed a new mouse model where AMPK catalytic activity can be deleted in a muscle-specific manner at a specific time point in adult mice. With this new model, we sought to clarify the direct role of AMPK in exercise-stimulated regulation of muscle metabolism.

2. MATERIALS AND METHODS

2.1. Generation of the tamoxifen-inducible muscle-specific AMPKα double knockout mouse model (AMPKα imdKO)

Inducible muscle-specific double AMPKα1/α2 KO mice (AMPKα imdKO) were generated by breeding double-floxed AMPKα1α2 mice (AMPKα1$^{fl/fl}$, AMPKα2$^{fl/fl}$) [15] with mice expressing a tamoxifen-inducible Cre-recombinase driven by the human skeletal actin promotor (HSA-MCM$^{+/-}$) [25]. Deletion of AMPKα1/α2 in skeletal muscle was achieved by intraperitoneal injection of tamoxifen (Cat. No. T5648, Sigma-Aldrich) dissolved in 99% ethanol and re-suspended in sunflower seed oil (Cat. No. S5007, Sigma-Aldrich). The tamoxifen treatment protocol consisted of three single injections (40 mg/kg body weight) each separated by 48 hours. Female double-floxed AMPKα1α2 control mice (AMPKα1$^{fl/fl}$, AMPKα2$^{fl/fl}$, HSA-MCM$^{-/-}$) and AMPKα imdKO (AMPKα1$^{fl/fl}$, AMPKα2$^{fl/fl}$, HSA-MCM$^{+/-}$) on a mixed background (C57/Bl6 87.5% and SV129 12.5%) were used in all experiments. Initially, a time course study was performed in order to determine the earliest time point for optimal deletion of skeletal muscle AMPKα protein. For this time course experiment mice were investigated 1, 3 and 8 weeks after the final tamoxifen injection and compared to vehicle-injected control mice (sunflower seed oil injections). 3 weeks after the last tamoxifen injection was the earliest time point with optimal deletion of AMPKα protein and therefore all following experiments were performed ~3 weeks after the final tamoxifen injection. Both AMPKα imdKO mice and AMPKα double-floxed control littermates aged 12 ± 5 weeks (means ± SD) were treated with tamoxifen. The tamoxifen administration protocol applied in the present study resulted in a substantial testicular swelling in male mice (unpublished observations) and we decided for ethical and experimental reasons to perform all following experiments in female mice only. All mice had free access to water and rodent chow and

were maintained on a 12:12 hour light-dark cycle. All experiments were approved by the Danish Animal Experiments Inspectorate (License #2013-15-2934-00911, #2014-15-2934-01037 and 2019-15-0201-01659) and complied with the EU guidelines for the protection of vertebra animals used for scientific purposes.

2.2. Body composition and morphological analyses

Body composition was measured prior to and ~3 weeks after final tamoxifen injection by the use of magnetic resonance imaging (EchoMRI 4-in-1; EchoMRI, Houston, TX). Skeletal muscle, heart, white adipose tissue, liver, and kidney were carefully dissected from anaesthetized control and AMPKα imdKO mice and visually inspected for any signs of disparity. Tissue mass was determined with 0.1 mg accuracy (ED124S, Sartorius, Goettingen, Germany).

2.3. Basal calorimetry

Prior to measurements, mice were acclimatized for 3 days to individually-housed airtight calorimetric cages connected to an indirect calorimetric system (Phenomaster/LabMaster system; TSE Systems, Bad Homburg, Germany). O_2 consumption (VO_2), CO_2 production (VCO_2), food intake and physical activity level (laser beam breaks) were recorded during a 48 hour period while the mice were receiving a chow diet (Altromin no. 1324; Brogaarden, Horsholm, Denmark) followed by a high fat diet (60% kcal derived from fat; no. D12492; Brogaarden, Horsholm, Denmark). After a 24-hour wash out period on regular chow diet the effect of 24 hours of fasting was investigated. For all calorimetric measurements mice were maintained on a 12 h:12 h light–dark cycle and housed at 20–21°C.

2.4. Treadmill acclimatization and maximal exercise capacity test

On 3 separate days (Pre, 1 week and 3 weeks after final tamoxifen injection), mice were adapted to a treadmill running system (TSE Systems). The adaptation protocol consisted of 5 min rest followed by 5 min running at 7.2 m/min and 5 min running at 9.6 m/min [16]. After one day of rest, a graded exercise capacity test was performed. The test was initiated by 5 min rest followed by treadmill running at 4.8 m/min with treadmill speed increased 2.4 m/min every 2 min at a 5° incline. Mice were forced to run by the use of pressurized air and an electric shocker grid at the back of the treadmill. Exhaustion was reached when the mice stayed on the shocking grid despite repeated agitation with pressurized air. The last passed speed level was defined as maximal running speed.

2.5. Substrate utilization during treadmill exercise

Substrate utilization during treadmill exercise was investigated at least 48 hours after the maximal exercise capacity test by measuring O_2 consumption (VO_2) and CO_2 production (VCO_2) in an airtight treadmill running system (CaloSys apparatus; TSE Systems, Germany). Mice were placed on the calorimetric treadmill and allowed to rest for 10 min. This was followed by a 5 min warm up at 40% of maximal treadmill running speed and 30 min continuous running at 60% of individual maximal running speed at a 5° incline. Measurements continued 15 min into exercise recovery.

2.6. Glucose uptake measurements during treadmill exercise

Mice either rested or exercised for 30 min at 70% of individual maximal running speed at a 15° incline. An intraperitoneal injection of saline containing [^{3}H]-2-deoxyglucose ([^{3}H]-2-DG) (8 ml/kg, 60 µCi/ml, Perkin Elmer, USA) was administered 20 min before the onset of exercise/rest. Blood samples in combination with blood glucose measurements (Contour XT, Bayer, Germany) were obtained from the tail vein immediately before and after exercise/rest to determine specific radioactivity in the blood. Mice were euthanized by cervical dislocation immediately after the last blood sample was drawn and tissues were quickly harvested and frozen in liquid nitrogen. Muscle 2-DG uptake was determined as [^{3}H]-2-deoxy-D-glucose-6-phosphate ([^{3}H]-2-DG-6-P) content by Somogyi and perchloric acid precipitations of muscle homogenate as previously described [16,26].

2.7. Glucose and insulin tolerance tests

For all tests, mice were individually housed. For the glucose tolerance test (GTT), mice were fasted for 5 hours in the morning before they were given an intraperitoneal injection of glucose (2 g/kg body weight) dissolved in a 0.9% saline solution. For the insulin tolerance test (ITT), overnight fed mice were fasted for 2 hours in the morning before they were given an intraperitoneal injection of insulin (1 U/kg body weight, Actrapid, Novo Nordisk, Bagsværd, Denmark). Blood was collected from the tail vein at 0, 20, 40, 60, 90, and 120 min in the GTT and 0, 20, 40, and 60 min in the ITT. Blood glucose concentrations were determined using a glucometer (Contour XT, Bayer, Germany). For the GTT, plasma insulin concentrations were determined at 0, 20, and 40 min using an enzyme-linked immunosorbent ELISA assay (Cat. No. 80-INSMSU-E10, ALPCO) according to the manufacturer's instructions.

2.8. Insulin- and contraction-stimulated glucose uptake in isolated muscles

Fed mice were anesthetized by an intraperitoneal injection of pentobarbital (10 mg/100 g body weight) before soleus and extensor digitorum longus (EDL) muscles were excised and suspended at resting tension in incubation chambers (model 610/820M, DMT, Denmark) containing Krebs-Ringer buffer (KRB) (117 mM NaCl, 4.7 mM KCl, 2.5 mM $CaCl_2$, 1.2 mM KH_2PO_4, 1.2 mM $MgSO_4$, 0.5 mM $NaHCO_3$, pH 7.4) supplemented with 0.1% bovine serum albumin (BSA), 2 mM Na-pyruvate, and 8 mM Mannitol. During the entire incubation period the buffer was maintained at 30°C and continuously gassed with carbogen (95% O_2 and 5% CO_2). After ~30 min pre-incubation, basal, submaximal (100 µU/ml), and maximal (10,000 µU/ml) insulin-stimulated muscle glucose uptake was determined during the last 10 min of a 30 min stimulation period by adding 1 mM [^{3}H]-2-DG (0.028 MBq/ml) and 7 mM [^{14}C]-Mannitol (0.0083 MBq/ml) to the incubation medium. For contraction-stimulated glucose uptake, the muscles were electrically stimulated to contract (1 s train/15 s, 0.2 ms pulses, 100 Hz, 30 V; MultiStim System-D330, Harvard Apparatus) for 10 min. 2-DG uptake during contraction was measured by adding 1 mM [^{3}H]-2-DG (0.028 MBq/ml) and 7 mM [^{14}C]-Mannitol (0.0083 MBq/ml) to the incubation medium immediately before initiation of muscle contraction. After incubation, the muscles were harvested, washed in ice-cold saline, blotted dry and quickly frozen in liquid nitrogen. Uptake of 2-DG was determined as previously described [27].

2.9. Contraction-stimulated FA oxidation in isolated soleus muscles

Contraction-stimulated exogenous palmitate oxidation in isolated soleus muscle was measured similarly as previously described [17]. In short, excised soleus muscles from anesthetized mice were mounted at resting tension (~5 mN) in vertical incubation chambers (Radnoti, Monrovia, CA)

containing 30°C oxygenated (95% O_2 and 5% CO_2) KRB supplemented with 5 mM glucose, 2% fat-free BSA, and 0.5 mM palmitate. After ~20 min of pre-incubation, the incubation buffer was replaced with KRB additionally containing [1-^{14}C]-palmitate (0.0044 MBq/ml). To seal off the incubation chambers, mineral oil (Cat. No. M5904, Sigma-Aldrich) was added on top. Exogenous palmitate oxidation was measured at rest and during 25 min contractions (18 trains/min, 0.6 s pulses, 30 Hz, 60 V). After incubation, incubation buffer and muscles were collected to determine the rate of palmitate oxidation as previously described [17,28]. Palmitate oxidation was determined as CO_2 production (complete FA oxidation) and acid-soluble metabolites (ASM, representing incomplete FA oxidation). As there was no difference in complete and incomplete FA oxidation between genotypes, palmitate oxidation is presented as a sum of these two forms.

2.10. Mitochondrial respiration of permeabilized skeletal muscle fibers

After excision, tibialis anterior (TA) muscles were immediately transferred to ice-cold BIOPS buffer (10 mM Ca-EGTA, 0.1 µM free Ca, 20 mM imidazole, 20 mM taurine, 50 mM K-MES, 0.5 mM DTT, 6.56 mM $MgCl_2$, 5.77 mM ATP, 15 mM phosphocreatine, pH 7.1). Adipose and connective tissue were removed, and muscle fibers were mechanically separated into small fiber bundles (~3 mg) with a fine forceps to maximize surface area and minimize diffusion limitations. Permeabilization of fiber bundles was ensured by 30 min saponin treatment (30 µg/mL in BIOPS) on a rotator at 4°C. After permeabilization, fiber bundles were washed at least 30 min in MiR05 buffer (0.5 mM EGTA, 3 mM $MgCl_2$, 60 mM K-lactobionate, 20 mM taurine, 10 mM KH_2PO_4, 20 mM Hepes, 110 mM sucrose, 1 g/L BSA, pH 7.1) before analyses. Mitochondrial respiration was measured in duplicates in permeabilized muscle fiber bundles under hyperoxic conditions ([O_2] ~400-200 µM) at 37°C in MiR05 medium using the Oxygraph-2k Oroboros Instruments, Innsbruck, Austria). Complex I supported leak

respiration was measured after addition of 5 mM pyruvate, 10 mM glutamate and 2 mM malate. Maximal Complex I supported oxidative phosphorylation (OXPHOS) capacity (CI_P) was measured after addition of ADP (4 mM). Complex I+II supported OXPHOS capacity ($CI+II_P$) was measured after succinate addition (10 mM). Electron transfer system (ETS) capacity through Complex I+II was measured after sequential addition of 0.5µM FCCP. Finally, ETS capacity through complex II (CII) was achieved by adding 1 uM rotenone to inhibit Complex I. After each respiration protocol, permeabilized fibers were extracted from the respiration chamber and weighed after vacuum drying and data are expressed as oxygen flux relative to muscle dry weight.

2.11. Muscle glycogen, nucleotide, AMPD activity and lactate measurements

Muscle glycogen content was determined by a fluorometric method as glycosyl units after acid hydrolysis of 10-15 mg wet weight muscle samples [29]. Muscle specimens from quadriceps muscle were extracted in perchloric acid and analyzed for nucleotides by reverse-phase HPLC. AMPD activity was measured in quadriceps muscle by adding 2 µl muscle homogenate to 1000 µl of the reagent solution containing 12.5 mM AMP and the formation of IMP was analyzed by HPLC. Kinetic properties for AMPD (V_{max} and K_m) were analyzed in muscle homogenate in the presence of 15 mM, 0.1 mM, 0.06 mM, and 0.04 mM AMP and the formation of IMP was quantified by HPLC as previously reported [30]. Muscle lactate concentration was determined in crushed quadriceps muscle by a fluorometric method as previously described [29].

2.12. mRNA isolation, reverse transcription and real time PCR.

A whole EDL muscle (~10 mg) and ~25 mg of quadriceps muscle were crushed in liquid nitrogen and subsequently homogenized before RNA was isolated by the guanidine thiocyanate (GT) phenol-chloroform method [31]. The pellet was washed twice in 75% EtOH (-20°C) and centrifuged for 5 min at 12,000 g and 4°C between washes. The pellet was vacuum dried after last wash and resuspended in 1 µl/(mg initial muscle) 0.1 mM EDTA. RNA concentration was determined using a Nanodrop1000 spectrophotometer (Thermo Fischer Scientific, Waltham, USA) and RNA purity was ensured by the 260/280 nm ratio. Reverse transcriptase reaction was performed on 3 µg of total RNA using the Superscript II RNase H- system (ThermoFisher Scientific, Waltham, USA) as previously described [32]. The mRNA content of specific genes was determined by fluorescence-based real time PCR (ABI PRISM 7900 Sequence Detection System, Applied Biosystems). The forward and reverse primers and TaqMan probes were either designed from mouse specific sequence data (Entrez-NIH and Ensembl, Sanger Institute) using computer software (Primer Express, Applied Biosystems) or purchased as kits from ThermoFisher Scientific. PCR amplification was performed in triplicates of 10 µl with 10 ng of cDNA as previously described [33] and with TATA Box Binding Protein (TBP) as endogenous control. TBP has previously been described as an endogenous reference gene [34] and we found TBP to be unaffected by the intervention and genotype in the present study. A detailed list of primer and probe sequences is given in supplemental 1. The cycle threshold (Ct) values of the unknown samples were converted to an amount by use of a relative standard curve derived from a dilution series of a representative pool. For each sample, the amount of specific genes analyzed was then divided by the amount of housekeeping gene (TBP) for assay normalization.

2.13. Muscle processing

Muscles were homogenizing in ice-cold buffer (10% glycerol, 20 mM Na-pyrophosphate, 150 mM NaCl, 50 mM Hepes 1% NP-40, 20 mM β-glycerophosphate, 10 mM NaF, 2 mM PMSF, 1 mM EDTA, 1 mM EGTA, 10 µg/ml aprotinin, 10 µg/ml leupeptin, 2 mM Na_3VO_4, and 3 mM benzamidine, pH 7.5) by the use of a TissueLyser II (QIAGEN, Hilden, Germany). Subsequently, homogenates were rotated end-over-end at 4°C for 1 hour. Muscle lysate was obtained as supernatant from homogenate by centrifugation for 20 min at 16,000 g and 4°C. Protein abundance in muscle homogenates and lysates was determined in triplicate by the bicinchoninic acid method with BSA as protein standards (Thermo Fisher Scientific, Waltham, USA).

2.14 Glycogen synthase (GS)-activity

GS-activity in muscle homogenates was measured in 96-well microtiter assay plates (Unifilter 350 plates; Whatman, Cambridge, UK) as previously described [35]. GS-activity is reported as percentage of fractional velocity (% FV) and was calculated as 100 x activity in the presence of 0.17 mM glucose-6-phosphate (G6P) divided by activity in the presence of 8 mM G6P (saturated).

2.15 SDS-PAGE and Western blotting

Muscle lysates were prepared in sample buffer and heated for 5 min at 96°C. Equal amounts of protein were loaded on self-cast gels and separated by the use of SDS-PAGE. Gels were transferred to polyvinylidene fluoride membranes (Merck, Darmstadt, Germany) using semidry blotting. Membranes were incubated for 5 min in TBST containing either 2% skim milk or 3% BSA and subsequently incubated overnight at 4°C with primary antibody. A detailed list of antibodies is given in the supplemental material (Supplemental 2). Proteins with bound primary and secondary antibody were

visualized by chemi-luminescence and a digital imaging system (ChemiDoc MP System, BioRad, California, USA). Linearity was assessed for all proteins in order to ensure that the obtained band intensity was within the dynamic range.

2.16 Statistical analyses

Data are presented as means ± SEM unless stated otherwise. Differences between AMPKα control and imdKO mice were analyzed by a Students t-test or 2-way ANOVA with or without repeated measurements as appropriate and specified in the figure legends. The Student-Newman-Keuls test was used for post hoc testing. Statistical analyses were performed in Sigmaplot (version13.0 ; SYSTAT, Erkrath, German) and $P < 0.05$ was chosen as significance level.

3. RESULTS

3.1 Time-course of skeletal muscle-specific deletion of AMPKα1 and α2

In order to define the earliest time-point at which full deletion of the catalytic AMPKα1 and α2 protein had occurred in myofibers, we investigated the AMPK subunit levels 1, 3 and 8 weeks after tamoxifen-induced gene deletion. 1 week after the last tamoxifen injection, the mRNA content of AMPKα1 and AMPKα2 in EDL muscle was reduced to ~58% and ~0%, respectively, compared to tamoxifen-treated AMPKα double-floxed control mice (Fig 1A and 1B). These changes in AMPKα gene expression were also present at the 8-week time-point and resulted in a marked reduction in AMPKα1 and near complete deletion in AMPKα2 protein content (Fig 1C-D and Supplementary Fig S3F). Thus, the AMPKα1 protein level was reduced to ~60% in AMPKα imdKO compared to control EDL muscle 1

week after tamoxifen treatment and dropped further reaching ~30% at 3 weeks after ended tamoxifen treatment (Fig 1C). The protein content of AMPKα2 in EDL muscle from AMPKα imdKO was reduced to ~30 and ~8% at 1 and 3 weeks following tamoxifen treatment, respectively (Fig 1D). A similar pattern for tamoxifen-induced reduction in AMPKα1 and AMPKα2 protein levels were also observed in quadriceps muscle (Supplementary Fig S3A-B). Importantly, protein levels of AMPKα1 and AMPKα2 in skeletal muscle from AMPKα imdKO mice measured 3 weeks after ended tamoxifen treatment correspond to levels observed in the previously described conventional (chronic) AMPKα muscle-specific double knockout (mdKO) mouse model [16] (right bar in Fig 1C-D). The remaining amount of AMPKα1 protein in whole muscle samples from AMPKα imdKO mice is also found in the conventional AMPKα mdKO model and likely derives from non-muscle cells (e.g. blood cells, adipocytes and endothelial cells) present in our crude muscle sample preparations. The expression in non-muscle cells is not expected to be affected due to the skeletal muscle specificity of the HSA promotor [16]. AMPKα1 and AMPKα2 protein levels in heart muscle remained similar between genotypes following tamoxifen treatment (Fig 1E-F and Supplementary Fig S3G), verifying that KO of the catalytic AMPK subunits indeed is specific for skeletal muscle myofibers. The AMPKβ2-associated heterotrimer complexes account for ~95% of the total AMPK pool in mouse EDL muscle (α2β2γ1 ~70%, α2β2γ3 ~20% and α1β2γ1 ~5%) [36], and in accordance the marked reduction in AMPKα muscle protein levels observed in the present model is accompanied by a corresponding reduction in protein levels of the regulatory AMPK subunits β2 and γ1, while AMPK γ3 only tended to be reduced (Supplementary Fig S3C-F). In absolute values, these protein levels resemble those seen in skeletal muscle of the conventional AMPKα mdKO mouse model.

342 Collectively, these data suggest that a maximal reduction in AMPKα1 and AMPKα2 protein levels is
343 observed at the earliest 3 weeks after ended tamoxifen treatment. Based on these observations the 3-
344 week time-point was chosen for all following experiments.

345 **3.2. Body composition and resting metabolism remain unaffected by inducible KO of AMPKα1**
346 **and α2 in skeletal muscle**

347 Body composition of control and AMPKα imdKO mice was investigated before and 3 weeks after
348 ended tamoxifen treatment by use of magnetic resonance scanning (Table 1). Before tamoxifen
349 treatment no differences between genotypes were noticed, both having normal growth rates and born
350 with the expected mendelian ratio (data not shown). A decrease in body weight (~3%) and an increase
351 in fat mass (~10%) were observed in both genotypes 3 weeks after tamoxifen relative to before
352 tamoxifen treatment. A minor decrease in lean body mass (~3%) was observed in AMPKα imdKO but
353 not control mice following tamoxifen treatment. However, no significant difference between genotypes
354 in lean body mass was evident before and after tamoxifen treatment. Careful dissection and weighing
355 of individual organs revealed similar weight and appearance of muscle, heart, adipose tissue, liver, and
356 kidney from AMPKα imdKO and control littermates (Table 2).
357 Resting metabolism during the light and dark period on chow diet was found to be comparable between
358 control and AMPKα imdKO mice (Supplementary Fig S4A-B). We also investigated the ability to
359 switch substrate utilization towards FA oxidation by subjecting the mice to 2 days of high fat diet
360 (HFD) and a 24 hours fasting regimen, respectively. The HFD intervention lowered RER from ~0.95 to
361 ~0.80 in both genotypes during the light period, and RER increased similarly in the two genotypes
362 during the dark period (RER from ~0.80 to ~0.85) (Supplementary Fig S4A and C). Compared to the
363 chow diet, the 24 hours fasting intervention lowered RER markedly in the light period and RER

364 declined further during the dark period (RER ~0.73 to ~0.71 in both genotypes) with no difference
365 between genotypes (Supplementary Fig S4D-E). Together, these data suggest that resting metabolism
366 under these experimental conditions is similarly covered by FA oxidation in AMPKα imdKO and
367 control mice. Oxygen consumption, spontaneous physical activity as well as food intake during the
368 different diet interventions showed no difference between AMPKα imdKO and control littermates
369 (Supplementary Fig S4F-P).

370 Collectively these observations demonstrate that body composition, resting metabolism and metabolic
371 flexibility, i.e. the ability to adjust metabolism according to different feeding and fasting regimes,
372 remain unaffected by conditional deletion of AMPKα subunits in skeletal muscle of adult mice.

373

374 **3.3. Normal whole body insulin action and insulin-stimulated glucose uptake in isolated skeletal**
375 **muscle from AMPKα imdKO mice**

376 Whole body insulin action and muscle insulin sensitivity were investigated to determine whether
377 inducible deletion of muscle AMPKα in adult mice was associated with development of insulin
378 resistance. Following an intraperitoneal glucose tolerance test (GTT), blood glucose concentration
379 increased similarly and showed a comparable dynamic response in the two genotypes (Fig 2A). Plasma
380 insulin concentrations, determined before as well as 20 and 40 min after the glucose challenge, were
381 also similar in the two genotypes (Fig 2B). An intraperitoneal insulin tolerance test (ITT) revealed
382 comparable whole body insulin action in the two genotypes (Fig 2C). Collectively, these data
383 demonstrate that both whole body insulin- and glucose-tolerance remain intact in mice with acute
384 deletion of AMPK activity in skeletal muscle myofibers. Because skeletal muscle is responsible for the

majority of glucose uptake during *in vivo* insulin stimulation [37], 2-DG uptake in isolated skeletal muscle was examined in the presence of a submaximal (100 µU/ml) and maximal (10,000 µU/ml) insulin concentration. Both submaximal and maximal insulin-stimulated glucose uptake in soleus and EDL muscles were comparable between AMPKα imdKO mice and control littermates (Fig 2D-E). In addition, insulin-stimulated signaling in EDL muscle at the level of Akt (Akt Thr308) and its downstream target TBC1D4 (TBC1D4 Thr642) were comparable between genotypes, suggesting that insulin signaling to GLUT4 translocation was regulated similarly in muscles from the two genotypes (Fig 2F-H). Overall, these findings demonstrate that acute deletion of AMPK catalytic activity in skeletal muscle does not affect whole body insulin action or the ability of insulin to stimulate glucose uptake in isolated skeletal muscle.

3.4. Inducible deletion of AMPKα in adult mice impairs running performance and lowers muscle glycogen content

In accordance with previous observations in mouse models with embryonic and hence chronic deletion of AMPK function in skeletal muscle [9,10,16,18], a reduction in maximal treadmill running speed was found in AMPKα imdKO mice relative to control littermates (Fig 3A). Interestingly, a ~15% reduction in maximal treadmill running speed was observed already 1 week after tamoxifen-induced AMPKα gene deletion and was still present 3 weeks after tamoxifen treatment. This early response to AMPKα gene deletion was also found for skeletal muscle glycogen content. Thus, glycogen concentration in quadriceps muscle was decreased by ~25% in AMPKα imdKO already 1 week after ended tamoxifen treatment and was still lower 3 and 8 weeks after tamoxifen treatment (Fig 3B). In order to evaluate whether the metabolic stress induced by treadmill exercise differed between genotypes, we measured muscle glycogen concentration before and after 30 min of treadmill exercise (Fig 3C). Although resting

muscle glycogen content was lower in AMPKα imdKO relative to control mice, the ability to utilize muscle glycogen (glycogen degradation) during treadmill exercise was similar between the two genotypes (Fig 3C). Moreover, activity of the glucose-incorporating enzyme - glycogen synthase (GS) - was elevated in muscle from AMPKα imdKO mice compared to control mice (Fig 3D). The content of key proteins involved in glucose uptake (GLUT4 and HKII) and glycogen degradation (glycogen phosphorylase (GP)) were similar in muscle from AMPKα imdKO and control mice. Interestingly, UDP-Glucose Pyrophosphorylase 2 (UGP2), but not GS protein content was lower in quadriceps muscle from AMPKα imdKO mice compared to control mice (Fig 3E). UGP2 is essential for glycogen synthesis as it generates UDP-glucose [38] to be incorporated into glycogen chains mainly catalyzed by GS. Analyses of the time course experiment revealed that UGP2 gene expression was reduced by ~40% in quadriceps muscle from AMPKα imdKO already 1 week after ended tamoxifen-induced AMPKα gene deletion (Fig 3F). This observation indicates that AMPK is involved in the regulation of UGP-2 gene expression and we hypothesize that the concurrent lowering of muscle glycogen content in muscle from AMPKα imdKO mice is related to this change in UGP-2 expression.

Taken together, these observations suggest that AMPK is required for treadmill running performance and for maintaining resting muscle glycogen content potentially via regulation of UGP2. On the contrary, the ability of skeletal muscle to use glycogen as an energy source during exercise remains unaffected. Because maximal running performance differed between genotypes the following treadmill running experiments were performed at a relative exercise intensity (% of maximal running capacity) of each individual mouse.

3.5 AMPK is required for maintaining muscle nucleotide balance during exercise

Exercise increases the turnover of ATP in skeletal muscle and ATP regeneration through adenylate kinase reaction is therefore important for maintaining cellular ATP levels. To avoid the accumulation of intracellular AMP, the muscle cell deaminates AMP to IMP catalyzed by the enzyme AMPD (Fig 4). Treadmill exercise for 30 min at the same relative intensity decreased muscle ATP levels in both genotypes, but to a greater extent in AMPKα imdKO mice than in control littermates (36% vs. 14% reduction in AMPKα imdKO and control mice, respectively) (Fig 5A). While muscle ADP content remained unaffected and similar in the two genotypes (Fig 5B), a significant increase in muscle AMP content was observed in response to treadmill exercise (Fig 5C). Interestingly, 30 min of treadmill exercise at the same relative intensity was associated with a 7-fold increase in IMP in muscle from AMPKα imdKO mice with no detectable increase in muscle from control littermates (Fig 5D). Lower ATP levels during exercise accompanied by accumulation of IMP suggest a disturbance in muscle energy balance when AMPKα imdKO mice perform treadmill exercise (Fig 4). Intracellular IMP, formed during exercise, can be degraded to inosine (INO) and hypoxanthine (HX), which can pass through the muscle cell membrane and hence can represent a potential loss of nucleotide precursors from the exercising muscle [39]. Adenosine (ADO) increased similarly in both genotypes in response to exercise ($p=0.16$ for main effect of exercise) (Fig 5E). However, both HX ($p=0.073$ for effect of genotype) and INO ($p=0.077$ for interaction between genotype and intervention) tended to be elevated in exercised muscle from AMPKα imdKO only (Fig 5F-G). Collectively, these findings suggest that AMPK is required for maintaining the skeletal muscle nucleotide balance during exercise. The enzyme adenosine monophosphate deaminase 1 (AMPD1) is highly expressed in skeletal muscle and catalyzes the deamination of AMP to IMP and therefore plays a key role in the purine nucleotide cycle. Interestingly, muscle AMPD enzyme activity (measured under saturated AMP concentrations) tended to increase in response to exercise in AMPKα imdKO, while remaining unchanged in muscle from

control littermates (p=0.08 for interaction between intervention and genotype) (Fig 5H). However, this could neither be explained by a genotype-dependent difference in kinetic properties in resting muscles (Table 3 and Suppl. Fig. S3K) or AMPD1 protein content (Fig 5I).

Collectively these data demonstrate that AMPK is necessary for maintaining the cellular nucleotide pool during exercise. Next, we investigated whether reduced ATP regeneration in muscle from AMPKα imdKO mice was related to impaired substrate uptake and/or utilization during exercise and muscle contraction.

3.6. Similar substrate utilization during exercise and muscle contraction in control and AMPKα imdKO mice

Substrate utilization in control and AMPKα imdKO mice during treadmill exercise was investigated at the same relative intensity (60% of individual maximal running speed). RER before exercise was comparable in the two genotypes (~0.72) and increased similarly during 30 min of treadmill exercise (averaged 0.78 ± 0.01 and 0.79 ± 0.01 for control and AMPKα imdKO mice, respectively) (Fig 6A). Upon cessation of exercise, RER declined to pre-exercise levels with no difference between genotypes. These findings suggest that exercise at the same relative intensity exerts a similar metabolic response in control and AMPKα imdKO mice. In accordance, measurement of exogenous palmitate oxidation in isolated soleus muscles revealed that FA oxidation was similar between genotypes at rest and increased to the same extent in response to electrically-stimulated muscle contractions (Fig 6B). Impaired FA oxidation in mice with chronic deletion of AMPK activity in skeletal muscle (AMPKα mdKO) has been associated with reduced expression of FA handling transport proteins (CD36 and FABPpm)

471 [16,40]. However, protein content of these FA transporters was similar in controls and AMPKα imdKO
472 mice (Fig 6C and Suppl. Fig. S3H).

473 A number of previous AMPK-deficient mouse models have reported impaired mitochondrial function
474 and/or expression of mitochondrial proteins [9,15,41]. In order to investigate the effect of AMPKα
475 deletion in adult mice on mitochondrial function, we measured mitochondrial respiration rates in
476 permeabilized fibers from TA muscle. Mitochondrial respiration was similar in the two genotypes
477 when analyzed in the successive presence of malate + glutamate + pyruvate (Leak), ADP (CI_P),
478 succinate ($CI+II_P$), FCCP (ETS CI+II), and rotenone (ETS CII) (Fig 6D). These observations are in
479 line with similar protein levels of subunits in complex I-V of the mitochondrial electron transport chain
480 (Fig 6E and Suppl. Fig. S3I).

481 Collectively, these findings suggest that the phenotypic trait of the previously described AMPK-
482 deficient mouse models is a consequence of chronic deletion that likely does not reflect the actual
483 consequence of lacking AMPK activity acutely in skeletal muscle.

484

485 **3.7. Normal muscle glucose uptake during *in vivo* exercise and *ex vivo* muscle contractions in**
486 **AMPKα imdKO mice**

487 Treadmill exercise for 30 min increased AMPK phosphorylation at Thr172, a surrogate marker for
488 AMPK activation, in quadriceps muscle from control mice, while this effect was absent in AMPKα
489 imdKO mice (Fig 7A and Suppl. Fig. S3J). Similarly, treadmill exercise increased phosphorylation of
490 TBC1D1 Ser231 in quadriceps muscle from control but not in muscle from AMPKα imdKO mice (Fig
491 7B). This observation was not due to a difference in TBC1D1 protein levels as these were similar in

quadriceps muscle from control and AMPKα imdKO mice. In the present study, we observed generally lowered phosphorylation of ACC Ser212 in muscle from AMPKα imdKO mice, while the ability to increase ACC Ser212 phosphorylation in response to exercise still was present (Fig 7C and Suppl. Fig. S3J). This may either suggest that other kinases than AMPK are capable of phosphorylating ACC Ser212 during exercise or alternatively that AMPK-induced phosphorylation of ACC Ser212 takes place in non-muscle cells that are present in our crude muscle sample preparations. Studies investigating contraction- and exercise-stimulated glucose uptake in skeletal muscle from various other AMPK-deficient mouse models suggest no or only a partial role of AMPK [9,12,14–16,42]. In conventional AMPKα mdKO mice, exercise is associated with markedly elevated blood glucose levels [16]. However, in the present study we found that 30 min of treadmill exercise resulted in a minor increase in blood glucose levels in both control and AMPKα imdKO mice that occurred concomitant with a similar increase in muscle lactate content (Fig 7D-E). Glucose uptake in TA, soleus, EDL and quadriceps muscle during exercise was similar between control and AMPKα imdKO mice (Fig 7F). These data demonstrate that muscle glucose uptake during *in vivo* exercise is not compromised by muscle-specific deletion of AMPK catalytic activity in adult mice. To further illuminate this matter, contraction-stimulated 2-DG uptake was assessed in isolated EDL and soleus muscles from control and AMPKα imdKO mice. During tetanic muscle contractions glucose uptake increased to a similar extent in isolated soleus and EDL muscles from control and AMPKα imdKO mice (Fig 7G-H). Muscle force development during this electrical stimulation protocol showed no difference between genotypes in EDL muscle (Suppl. Fig. S5A), but was significantly lower (~23% lower at all time points) in soleus muscle ($p=0.049$) from AMPKα imdKO mice compared to control littermates (Suppl. Fig. S5B). Thus, albeit force development was generally lower for soleus muscle from AMPKα imdKO, the decline in force development over time (fatigue) showed a similar pattern in both genotypes. Force development

515 during electrically stimulated single twitch stimulation resulted in comparable force development
516 (Suppl. Fig S5C). *Ex vivo* contractions increased phosphorylation of AMPKα Thr172 in control EDL
517 and soleus muscles, while phosphorylation of AMPKα Thr172 in AMPKα imdKO muscle at rest was
518 reduced and did only increase modestly in soleus muscle in response to contractions (Suppl. Fig S5D-E
519 and S5J). Both basal and contraction-stimulated phosphorylation of AMPK downstream targets, ACC
520 Ser212 and TBC1D1 Ser231, were reduced in EDL muscle from AMPKα imdKO mice (Suppl. Fig
521 S5F-G and S5J). However, in response to contractions, phosphorylation of ACC Ser212 and TBC1D1
522 Ser231 in soleus muscle increased similarly in both genotypes (Suppl. Fig S5H-J). ACC and TBC1D1
523 protein levels in soleus were comparable in control and AMPKα imdKO mice (data not shown), while
524 TBC1D1 protein content was lower (~25%,) in EDL muscle from AMPKα imdKO mice compared to
525 control mice (data not shown).

526 Collectively, these data demonstrate that AMPK is dispensable for contraction-stimulated glucose
527 uptake in skeletal muscle and that the signaling axis leading to increased glucose uptake, at least in
528 glycolytic quadriceps and EDL muscles, can be mediated independently of TBC1D1
529 phosphoregulation.

530

531 **4. DISCUSSION**

532 The central role of AMPK as a gatekeeper in the regulation of skeletal muscle metabolism is mainly
533 based on AMPK-deficient mouse models with chronic lack of AMPK function. However, results
534 derived from such models are potentially biased by confounding adaptations due to the life-long
535 AMPK deficiency (including embryonic development), as emphasized by marked defects in metabolic

proteins, mitochondrial function and extreme exercise intolerance in some of these conventional models. In an attempt to minimize the influence of these confounding factors and to study the direct and acute effect of AMPK deficiency, we generated a new transgenic mouse model with tamoxifen-inducible muscle-specific deletion of catalytic AMPK activity in adult mice (AMPKα imdKO).

It has previously been reported that whole body deletion of AMPKα2 leads to a greater degradation of ATP in skeletal muscle during exercise and is associated with accumulation of AMP and IMP [43]. However, in that study the whole body AMPKα2 KO mice performed exercise at the same absolute intensity as the control littermates. Today, we know that these findings were biased, as the maximal running capacity of this KO model is reduced compared to WT control mice. Therefore, these observations may be related to a difference in exercise workload between genotypes rather than a direct consequence of a lack in AMPK activity. Notably, Lee-Young and co-workers reported accelerated ATP degradation but similar AMP concentrations during exercise in muscle from AMPKα2 KD mice compared to control mice, although exercise was performed at the same relative exercise intensity [10]. The study also reported a marked impairment in mitochondrial respiratory capacity (~32 and 50% impairment in complex I and IV activities, respectively) and it could therefore be speculated that the accelerated ATP depletion in muscle from AMPKα2 KD mice was the results of a reduced capacity for aerobic ATP repletion due to mitochondrial dysfunction. In the present study, ATP degradation was also accelerated in muscle from AMPKα imdKO mice despite intact mitochondrial function and despite that these mice were running at the same relative exercise intensity. This clearly suggests that AMPK activation during exercise is necessary for maintaining myocellular ATP levels during exercise. The greater ATP degradation during exercise in combination with lower muscle glycogen content in AMPKα imdKO mice may also explain the lower maximal running speed observed

in these mice. In contrast to previous studies, these observations were independent of muscle glucose uptake, substrate utilization and mitochondrial function.

The role of AMPK in the regulation of substrate utilization during exercise has been investigated in different mouse models with chronic deletion of AMPK activity [9,16,17,44]. AMPKβ1β2M-KO mice show increased reliance on FA oxidation during exercise (decreased RER) [9], but direct interpretation of this observation is compromised by extreme exercise intolerance (~57% reduction in maximal running speed) and hence dramatically absolute lower running speed during treadmill exercise. In contrast, deletion of both AMPKα isoforms (AMPKα mdKO) or the upstream kinase LKB1 (LKB1 KO) in skeletal muscle results in increased reliance on glucose utilization during exercise (increased RER) [16,17]. This may be a consequence of impaired FA oxidation due to lowered expression of fat transport proteins (e.g. CD36 and FABPpm) and lowered mitochondrial capacity/enzyme activity reported for these mice [15–17]. In the current study, we observed normal substrate utilization during *in vivo* exercise and *ex vivo* contractions of isolated muscles as well as intact expression of fatty acid transporter proteins and mitochondrial respiratory function. Collectively, this supports the notion that alterations in substrate utilization in mouse models with chronic deletion of AMPK activity are due to persistent alterations in the protein expression profile, mitochondrial function or extreme exercise intolerance rather than consequences of lacking acute AMPK-related regulation.

One of the proposed roles of AMPD is to prevent a large increase in ADP by removing AMP, hereby favoring ATP formation by the adenylate kinase reaction [45]. Thus, we interpret the trend towards increased AMPD activity and massive formation of IMP in skeletal muscle from AMPKα imdKO mice during exercise as a protective mechanism to avoid accumulation of AMP. *In vitro* studies have reported that AMPD activity is enhanced during muscle contractions in correspondence with

elevated H^+ as a result of lactate formation [46,47]. However, muscle lactate concentration increased similarly in response to exercise in control and AMPKα imdKO mice, suggesting that other factors than muscle H^+ accumulation contribute to the elevated AMPD activity in muscle from AMPKα imdKO mice. For *in vitro* AMPD activity measurements, the muscle homogenate was diluted ~500 fold for the assay procedure, likely eliminating possible influence of soluble factors present in the muscle. This suggests the presence of a regulation *in vivo* during exercise in AMPKα imdKO mice that is preserved during *in vitro* AMPD activity measurements. Phosphatase treatment has been shown to alter affinity of AMPD for its substrate AMP while the V_{max} remains unchanged [30]. This suggests that other allosteric regulations than protein phosphorylation have increased maximal AMPD activity in muscle from exercising AMPKα imdKO mice in the present study.

While AMPK activation by pharmacological means demonstrates that AMPK is sufficient to increase muscle glucose uptake [6–8], the proposed necessary role of AMPK in the regulation of contraction-stimulated muscle glucose uptake has been studied intensively in various transgenic mouse models with conflicting findings. Some studies have reported intact glucose uptake during *ex vivo* muscle contractions [13,15,19,20,22], while other studies have reported a partially decreased ability to increase muscle glucose uptake in response to contractile activity under some experimental conditions [9,11–15]. Moreover, glucose uptake during exercise is impaired in AMPKβ1β2M-KO mice but remains intact in AMPKα mdKO and LKB1-KO mice [9,16,17]. In the current study, we used an inducible AMPKα KO mouse model and observed that AMPK is dispensable for regulating glucose uptake in response to *in vivo* exercise and *ex vivo* muscle contractions.

TBC1D1 has been suggested to be involved in AMPK-mediated signaling that regulates GLUT4 translocation to increase muscle glucose uptake during muscle contractions [48]. A number of

602 studies have reported reduced phosphorylation of TBC1D1 at Ser231 in muscle of AMPK-deficient
603 mice in response to muscle contractions [9,16,49–51]. Moreover, muscle from TBC1D1-deficient
604 mouse models show reduced contraction- and exercise-stimulated glucose uptake [52–54], suggesting
605 that the AMPK-TBC1D1 signaling axis is required for regulating glucose uptake during exercise.
606 However, the TBC1D1 KO mouse model is associated with impaired GLUT4 expression in skeletal
607 muscle, complicating the overall interpretation of those findings. Overexpression of TBC1D1 mutated
608 to alanine at four phosphorylation sites in skeletal muscle (Ser231Ala, Thr499Ala, Thr590Ala and
609 Ser621Ala) seems not to affect GLUT4 protein content and is still associated with a marked reduction
610 (22%) in contraction-stimulated glucose transport [55]. In contrast, mutation of a single
611 phosphorylation site on TBC1D1 (Ser231Ala) does not compromise contraction- and exercise-
612 stimulated glucose uptake [56]. In the present study, contraction-stimulated TBC1D1 phosphorylation
613 at Ser231 did not increase in glycolytic muscles (quadriceps and EDL) from AMPKα imdKO mice,
614 albeit muscle glucose uptake increased similarly in both genotypes. Recently, our research group has
615 clarified these seemingly discrepant findings of AMPK-TBC1D1 signaling in regard to contraction-
616 stimulated muscle glucose uptake. Thus, we convincingly show that AMPK and TBC1D1 are
617 necessary and important for maintaining glucose uptake elevated in skeletal muscle in the immediate
618 period after, but not during, exercise and contraction [57]. Altogether, these findings support the
619 concept that glucose uptake can be regulated independently of TBC1D1 phosphorylation at Ser231, and
620 it could be speculated that muscle contractile activity leads to an activation of a broad range of
621 intracellular signaling events that promote glucose uptake and fat oxidation during exercise
622 independently of AMPK.

All experiments in this study were performed at room temperature and hence below mouse thermoneutrality. Recent evidence suggests that mild cold stress induced by ambient housing may confound the experimental outcome in mice [58]. However, McKie and colleagues observed that exercise-induced gene-expression and AMPK activation in muscle were comparable between experiments performed at room temperature and thermoneutrality [59]. This indicates that at least the acute exercise responses in skeletal muscle in the current study likely also would have been observed at thermoneutrality.

Interestingly, the promptly reduced muscle glycogen content (1 wk after ended tamoxifen treatment) in AMPKα imdKO mice was accompanied by a corresponding reduction in UGP2 gene expression. Support for a direct link between AMPK activation and UGP2 gene expression has been provided by transcriptomic profiling (microarray analysis) of muscles from AMPKγ3^{R225Q} transgenic mice, AMPKγ3$^{-/-}$ knockout mice, and AICAR-treated wild-type mice [60]. Thus, increased AMPK activity, either by introducing an activating AMPKγ3 mutation (AMPKγ3^{R225Q}) or AMPK activation by AICAR, induced an increase in UGP2 gene expression while genetic deletion of AMPKγ3 (AMPKγ3$^{-/-}$) induced a corresponding reduction. Furthermore, the AMPKγ3 gain of function mutation in pig muscle (AMPKγ3^{R200Q}) leads to a 3-fold increase in UGP2 protein levels [61]. Based on mutational cell studies, GS is considered rate-limiting for glycogen synthesis and UGP2 has generally been considered to play a minor role for glycogen storage [62]. However, we speculate that UGP2 may contribute to glycogen storage capacity by promoting glucose flux towards GS and explain the lower muscle glycogen content in AMPKα imdKO mice.

In conclusion, we have generated a new mouse model with inducible skeletal muscle-specific deletion of the catalytic AMPKα subunits in adult mice that allows us to study the direct effect(s) of AMPK in muscle metabolism. Acute deletion of AMPK activity in adult mouse muscle reveals that intracellular mediators other than AMPK are sufficient to regulate glucose uptake and substrate utilization in response to exercise and muscle contractions. However, AMPK is central for maintaining cellular nucleotide balance during exercise, as an increased deamination of AMP to IMP is observed in muscle from AMPKα imdKO mice during exercise. Moreover, acute deletion of muscle AMPKα in adult mice promptly reduces muscle glycogen content and lowers UGP2 expression. These observations likely explain the lower maximal treadmill running capacity in AMPKα imdKO observed already 1 week after AMPKα gene deletion.

Funding sources: The study was supported by grants (FSS 8020-00288 / 6110 00498B) from Danish Council for Independent Research, Medical Sciences (to J.F.P.W.), the Novo Nordisk Foundation (NNF16OC0023046) (to J.F.P.W.), and the Lundbeck Foundation (R266-2017-4358) (to J.F.P.W.). This work was supported by a research grant (to R.K. and A.M.F.) from the Danish Diabetes Academy, which is funded by the Novo Nordisk Foundation, grant number NNF17SA0031406.

Declaration of interest: none.

Acknowledgements: The authors acknowledge the skilled technical help provided by Karina Olsen, Betina Bolmgren, Nicoline Resen Andersen, Irene Beck Nielsen (Department of Nutrition, Exercise, and Sports, Faculty of Science, University of Copenhagen) and Anja Jokipi-Utzon (Institute of Sports Medicine Copenhagen, Bispebjerg Hospital). We also thank Karyn A. Esser (Department of Physiology and Functional Genomics, University of Florida, Gainesville, United States) for providing mice carrying inducible human skeletal actin (HSA)-Cre. The authors acknowledge the antibodies kindly provided by Prof. Olga Göransson, Lund University; Prof. Graham Hardie, Dundee University; Dr. Calles-Escandon, Wake Forest University and Prof. Oluf Pedersen, University of Copenhagen.

REFERENCES

[1] Holloszy, J.O., Kohrt, W.M., 1996. Regulation of Carbohydrate and Fat Metabolism During and After Exercise. Annu Rev Nutr. 16: 121–38.

[2] Richter, E.A., Ruderman, N.B., 2009. AMPK and the biochemistry of exercise: implications for human health and disease. Biochemical Journal 418(2): 261–75, Doi: 10.1042/BJ20082055.

[3] Hardie, D.G., Sakamoto, K., 2006. AMPK: a key sensor of fuel and energy status in skeletal muscle. Physiology 21: 48–60, Doi: 10.1152/physiol.00044.2005.

[4] Corton, J.M., Gillespie, J.G., Hardie, D.G., 1994. Role of the AMP-activated protein kinase in the cellular stress response. Current Biology : CB 4(4): 315–24, Doi: 10.1016/S0960-9822(00)00070-1.

[5] Winder, W.W., Hardie, D.G., 1999. AMP-activated protein kinase, a metabolic master switch: Possible roles in Type 2 diabetes. American Journal of Physiology - Endocrinology and Metabolism 277(1): E1–10, Doi: 10.1152/ajpendo.1999.277.1.e1.

[6] Cokorinos, E.C., Delmore, J., Reyes, A.R., Albuquerque, B., Kjøbsted, R., Jørgensen, N.O., et al., 2017. Activation of Skeletal Muscle AMPK Promotes Glucose Disposal and Glucose Lowering in Non-human Primates and Mice. Cell Metabolism 25(5): 1147-1159.e10, Doi: 10.1016/j.cmet.2017.04.010.

[7] Merrill, G.F., Kurth, E.J., Hardie, D.G., Winder, W.W., 1997. AICA riboside increases AMP-activated protein kinase, fatty acid oxidation, and glucose uptake in rat muscle. The American Journal of Physiology 273(6): E1107-12, Doi: 10.1152/ajpendo.1997.273.6.E1107.

[8] Myers, R.W., Guan, H.P., Ehrhart, J., Petrov, A., Prahalada, S., Tozzo, E., et al., 2017. Systemic pan-AMPK activator MK-8722 improves glucose homeostasis but induces cardiac hypertrophy. Science 357(6350): 507–11, Doi: 10.1126/science.aah5582.

[9] O'Neill, H.M., Maarbjerg, S.J., Crane, J.D., Jeppesen, J., Jørgensen, S.B., Schertzer, J.D., et al., 2011. AMP-activated protein kinase (AMPK) beta1beta2 muscle null mice reveal an essential role for AMPK in maintaining mitochondrial content and glucose uptake during exercise. Proceedings of the National Academy of Sciences of the United States of America 108(38): 16092–7, Doi: 10.1073/pnas.1105062108.

[10] Lee-Young, R.S., Griffee, S.R., Lynes, S.E., Bracy, D.P., Ayala, J.E., McGuinness, O.P., et al., 2009. Skeletal muscle AMP-activated protein kinase is essential for the metabolic response to exercise in vivo. J Biol Chem 284(36): 23925–34, Doi: M109.021048 [pii]\r10.1074/jbc.M109.021048.

[11] Jørgensen, S.B., Viollet, B., Andreelli, F., Frøsig, C., Birk, J.B., Schjerling, P., et al., 2004. Knockout of the α2 but Not α1, 5′-AMP-activated Protein Kinase Isoform Abolishes 5-Aminoimidazole-4-carboxamide-1-β-4-ribofuranoside- but Not Contraction-induced Glucose Uptake in Skeletal Muscle. Journal of Biological Chemistry 279(2): 1070–9, Doi: 10.1074/jbc.M306205200.

[12] Mu, J., Brozinick, J.T., Valladares, O., Bucan, M., Birnbaum, M.J., 2001. A role for AMP-activated protein kinase in contraction- and hypoxia-regulated glucose transport in skeletal muscle. Molecular Cell 7(5): 1085–94, Doi: 10.1016/S1097-2765(01)00251-9.

[13] Jensen, T.E., Schjerling, P., Viollet, B., Wojtaszewski, J.F.P., Richter, E. a., 2008. AMPK α1 activation is required for stimulation of glucose uptake by twitch contraction, but not by H2O2, in mouse skeletal

717 muscle. PLoS ONE 3(5), Doi: 10.1371/journal.pone.0002102.

718 [14] Lefort, N., St-Amand, E., Morasse, S., Cote, C.H., Marette, A., 2008. The alpha-subunit of AMPK is
719 essential for submaximal contraction-mediated glucose transport in skeletal muscle in vitro. American
720 Journal of Physiology. Endocrinology and Metabolism 295(6): E1447-54, Doi:
721 10.1152/ajpendo.90362.2008.

722 [15] Lantier, L., Fentz, J., Mounier, R., Leclerc, J., Treebak, J.T., Pehmoller, C., et al., 2014. AMPK controls
723 exercise endurance, mitochondrial oxidative capacity, and skeletal muscle integrity. The FASEB Journal
724 28(7): 3211–24, Doi: 10.1096/fj.14-250449.

725 [16] Fentz, J., Kjøbsted, R., Birk, J.B., Jordy, A.B., Jeppesen, J., Thorsen, K., et al., 2015. AMPKα is critical
726 for enhancing skeletal muscle fatty acid utilization during in vivo exercise in mice. The FASEB Journal
727 29(5): 1725–38, Doi: 10.1096/fj.14-266650.

728 [17] Jeppesen, J., Maarbjerg, S.J., Jordy, A.B., Fritzen, A.M., Pehmøller, C., Sylow, L., et al., 2013. LKB1
729 regulates lipid oxidation during exercise independently of AMPK. Diabetes 62(5): 1490–9, Doi:
730 10.2337/db12-1160.

731 [18] Maarbjerg, S.J., Jørgensen, S.B., Rose, A.J., Jeppesen, J., Jensen, T.E., Treebak, J.T., et al., 2009. Genetic
732 impairment of AMPK alfa2 signaling does not reduce muscle glucose uptake during treadmill exercise in
733 mice. American Journal of Physiology - Endocrinology and Metabolism 297: 924–34, Doi:
734 10.1152/ajpendo.90653.2008.

735 [19] Barnes, B.R., Marklund, S., Steiler, T.L., Walter, M., Hjälm, G., Amarger, V., et al., 2004. The 5'-AMP-
736 activated protein kinase gamma3 isoform has a key role in carbohydrate and lipid metabolism in
737 glycolytic skeletal muscle. The Journal of Biological Chemistry 279(37): 38441–7, Doi:
738 10.1074/jbc.M405533200.

739 [20] Steinberg, G.R., O'Neill, H.M., Dzamko, N.L., Galic, S., Naim, T., Koopman, R., et al., 2010. Whole
740 body deletion of AMP-activated protein kinase β2 reduces muscle AMPK activity and exercise capacity.
741 The Journal of Biological Chemistry 285(48): 37198–209, Doi: 10.1074/jbc.M110.102434.

742 [21] Fujii, N., Hirshman, M.F., Kane, E.M., Ho, R.C., Peter, L.E., Seifert, M.M., et al., 2005. AMP-activated
743 protein kinase alpha2 activity is not essential for contraction- and hyperosmolarity-induced glucose
744 transport in skeletal muscle. The Journal of Biological Chemistry 280(47): 39033–41, Doi:
745 10.1074/jbc.M504208200.

746 [22] Merry, T.L., Steinberg, G.R., Lynch, G.S., McConell, G.K., 2010. Skeletal muscle glucose uptake during
747 contraction is regulated by nitric oxide and ROS independently of AMPK. American Journal of
748 Physiology. Endocrinology and Metabolism 298(3): E577–85, Doi: 10.1152/ajpendo.00239.2009.

749 [23] Kjøbsted, R., Hingst, J.R., Fentz, J., Foretz, M., Sanz, M.-N., Pehmøller, C., et al., 2018. AMPK in
750 skeletal muscle function and metabolism. The FASEB Journal 32(4): 1741–77, Doi:
751 10.1096/fj.201700442R.

752 [24] Tullson, C., Whitlock, M., Terjung, R., 1990. Adenine nucleotide degradation in slow-twitch red muscle.
753 American Journal of Physiology 258(2): 258–65, Doi: 10.1152/ajpcell.1990.258.2.C258.

754 [25] McCarthy, J.J., Srikuea, R., Kirby, T.J., Peterson, C.A., Esser, K.A., 2012. Inducible Cre transgenic
755 mouse strain for skeletal muscle-specific gene targeting. Skeletal Muscle 2(1): 8, Doi: 10.1186/2044-

5040-2-8.

[26] Somogyi, M., 1945. DETERMINATION OF BLOOD SUGAR. J. Biol. Chem. 160: 69–73.

[27] Kjøbsted, R., Treebak, J.T., Fentz, J., Lantier, L., Viollet, B., Birk, J.B., et al., 2015. Prior AICAR Stimulation Increases Insulin Sensitivity in Mouse Skeletal Muscle in an AMPK-Dependent Manner. Diabetes 64(6): 2042–55, Doi: 10.2337/db14-1402.

[28] Steinberg, G.R., Bonen, A., Dyck, D.J., 2002. Fatty acid oxidation and triacylglycerol hydrolysis are enhanced after chronic leptin treatment in rats. American Journal of Physiology - Endocrinology and Metabolism 282(3 45-3): 593–600, Doi: 10.1152/ajpendo.00303.2001.

[29] Lowry, O.H., Passonneau, J.V., 1972. A Flexible System of Enzymatic Analysis. London: Academic Press, Inc.

[30] Tullson, P.C., Rush, J.W.E., Wieringa, B., Terjung, R.L., 1998. Alterations in AMP deaminase activity and kinetics in skeletal muscle of creatine kinase-deficient mice. American Journal of Physiology - Cell Physiology 274(5): C1411–6, Doi: 10.1152/ajpcell.1998.274.5.c1411.

[31] Chomczynski, P., Sacchi, N., 1987. Single-step method of RNA isolation by acid guanidinium thiocyanate-phenol-chloroform extraction. Analytical Biochemistry 162(1): 156–9, Doi: 10.1016/0003-2697(87)90021-2.

[32] Hildebrandt, A.L., Neufer, P.D., 2000. Exercise attenuates the fasting-induced transcriptional activation of metabolic genes in skeletal muscle. American Journal of Physiology - Endocrinology and Metabolism 278(6): E1078-86, Doi: 10.1152/ajpendo.2000.278.6.E1078.

[33] Lundby, C., Nordsborg, N., Kusuhara, K., Kristensen, K.M., Neufer, P.D., Pilegaard, H., 2005. Gene expression in human skeletal muscle: Alternative normalization method and effect of repeated biopsies. European Journal of Applied Physiology 95(4): 351–60, Doi: 10.1007/s00421-005-0022-7.

[34] Gong, H., Sun, L., Chen, B., Han, Y., Pang, J., Wu, W., et al., 2016. Evaluation of candidate reference genes for RT-qPCR studies in three metabolism related tissues of mice after caloric restriction. Scientific Reports 6(6): 38513 (p1-12), Doi: 10.1038/srep38513.

[35] Højlund, K., Birk, J.B., Klein, D.K., Levin, K., Rose, A.J., Hansen, B.F., et al., 2009. Dysregulation of glycogen synthase COOH- and NH2-terminal phosphorylation by insulin in obesity and type 2 diabetes mellitus. Journal of Clinical Endocrinology and Metabolism 94(11): 4547–56, Doi: 10.1210/jc.2009-0897.

[36] Treebak, J.T., Birk, J.B., Hansen, B.F., Olsen, G.S., Wojtaszewski, J.F.P., 2009. A-769662 activates AMPK beta1-containing complexes but induces glucose uptake through a PI3-kinase-dependent pathway in mouse skeletal muscle. American Journal of Physiology. Cell Physiology 297(4): C1041–52, Doi: 10.1152/ajpcell.00051.2009.

[37] Shulman, G.I., Rothman, D.L., Jue, T., Stein, P., DeFronzo, R.A., Shulman, R.G., 1990. Quantitation of muscle glycogen synthesis in normal subjects and subjects with non-insulin-dependent diabetes by 13C nuclear magnetic resonance spectroscopy. The New England Journal of Medicine 322(4): 223–8, Doi: 10.1056/NEJM199001253220403.

[38] Roach, P.J., Depaoli-roach, A.A., Hurley, T.D., Tagliabracci, V.S., 2012. Glycogen and its metabolism:

some new developments and old themes. Biochemical Journal 441(3): 763–87, Doi: 10.1042/BJ20111416.

[39] Hellsten, Y., Richter, E.A., Kiens, B., Bangsbo, J., 1999. AMP deamination and purine exchange in human skeletal muscle during and after intense exercise. Journal of Physiology 520(3): 909–20, Doi: 10.1111/j.1469-7793.1999.00909.x.

[40] Fentz, J., Kjøbsted, R., Kristensen, C.M., Hingst, J.R., Birk, J.B., Gudiksen, A., et al., 2015. AMPKα is essential for acute exercise-induced gene responses but not for exercise training-induced adaptations in mouse skeletal muscle. American Journal of Physiology - Endocrinology And Metabolism 309(11): E900-914, Doi: 10.1152/ajpendo.00157.2015.

[41] Kristensen, J.M., Larsen, S., Helge, J.W., Dela, F., Wojtaszewski, J.F.P., 2013. Two Weeks of Metformin Treatment Enhances Mitochondrial Respiration in Skeletal Muscle of AMPK Kinase Dead but Not Wild Type Mice. PLoS ONE 8(1): 1–10, Doi: 10.1371/journal.pone.0053533.

[42] Jørgensen, S.B., Viollet, B., Andreelli, F., Frøsig, C., Birk, J.B., Schjerling, P., et al., 2004. Knockout of the alpha2 but not alpha1 5'-AMP-activated protein kinase isoform abolishes 5-aminoimidazole-4-carboxamide-1-beta-4-ribofuranosidebut not contraction-induced glucose uptake in skeletal muscle. The Journal of Biological Chemistry 279(2): 1070–9, Doi: 10.1074/jbc.M306205200.

[43] Jørgensen, S.B., Wojtaszewski, J.F.P., Viollet, B., Andreelli, F., Birk, J.B., Hellsten, Y., et al., 2005. Effects of α-AMPK knockout on exercise-induced gene activation in mouse skeletal muscle. FASEB Journal 19(9): 1–26, Doi: 10.1096/fj.04-3144fje.

[44] Fritzen, A.M., Lundsgaard, A.-M., Jeppesen, J., Christiansen, M.L.B., Biensø, R., Dyck, J.R.B., et al., 2015. 5′-AMP activated protein kinase α_2 controls substrate metabolism during post-exercise recovery via regulation of pyruvate dehydrogenase kinase 4. The Journal of Physiology 593(21): 4765–80, Doi: 10.1113/JP270821.

[45] Norman, B., Hellsten-Westing, Y., Sjödin N, B., Jansson, E., 1994. AMP deaminase in skeletal muscle of healthy males quantitatively determined by new assay. Acta Physiologica Scandinavica 150(4): 397–403, Doi: 10.1111/j.1748-1716.1994.tb09704.x.

[46] Lowenstein, J.M., 1990. The purine nucleotide cycle revised. International Journal of Sports Medicine 11: S37–46, Doi: 10.1055/s-2007-1024853.

[47] Dudley, G.A., Terjung, R.L., 1985. Influence of acidosis on AMP deaminase activity in contracting fast-twitch muscle. The American Journal of Physiology 248(1 Pt 1): C43-50, Doi: 10.1152/ajpcell.1985.248.1.C43.

[48] Chavez, J.A., Roach, W.G., Keller, S.R., Lane, W.S., Lienhard, G.E., 2008. Inhibition of GLUT4 translocation by Tbc1d1, a Rab GTPase-activating protein abundant in skeletal muscle, is partially relieved by AMP-activated protein kinase activation. Journal of Biological Chemistry 283(14): 9187–95, Doi: 10.1074/jbc.M708934200.

[49] Treebak, J.T., Pehmøller, C., Kristensen, J.M., Kjøbsted, R., Birk, J.B., Schjerling, P., et al., 2014. Acute exercise and physiological insulin induce distinct phosphorylation signatures on TBC1D1 and TBC1D4 proteins in human skeletal muscle. The Journal of Physiology 592(2): 351–75, Doi: 10.1113/jphysiol.2013.266338.

[50] Pehmoller, C., Treebak, J.T., Birk, J.B., Chen, S., Mackintosh, C., Hardie, D.G., et al., 2009. Genetic disruption of AMPK signaling abolishes both contraction- and insulin-stimulated TBC1D1 phosphorylation and 14-3-3 binding in mouse skeletal muscle. Am J Physiol Endocrinol Metab 297(3): E665-75, Doi: 10.1152/ajpendo.00115.2009.

[51] Vichaiwong, K., Purohit, S., An, D., Toyoda, T., Jessen, N., Hirshman, M.F., et al., 2010. Contraction regulates site-specific phosphorylation of TBC1D1 in skeletal muscle. Biochemical Journal 431(2): 311–20, Doi: 10.1042/BJ20101100.

[52] Szekeres, F., Chadt, A., Tom, R.Z., Deshmukh, A.S., Chibalin, A. V., Björnholm, M., et al., 2012. The Rab-GTPase-activating protein TBC1D1 regulates skeletal muscle glucose metabolism. American Journal of Physiology. Endocrinology and Metabolism 303(4): E524-33, Doi: 10.1152/ajpendo.00605.2011.

[53] Dokas, J., Chadt, A., Nolden, T., Himmelbauer, H., Zierath, J.R., Joost, H.G., et al., 2013. Conventional knockout of Tbc1d1 in mice impairs insulin- and AICAR-stimulated glucose uptake in skeletal muscle. Endocrinology 154(10): 3502–14, Doi: 10.1210/en.2012-2147.

[54] Stöckli, J., Meoli, C.C., Hoffman, N.J., Fazakerley, D.J., Pant, H., Cleasby, M.E., et al., 2015. The RabGAP TBC1D1 plays a central role in exercise-regulated glucose metabolism in skeletal muscle. Diabetes 64(6): 1914–22, Doi: 10.2337/db13-1489.

[55] An, D., Toyoda, T., Taylor, E.B., Yu, H., Fujii, N., Hirshman, M.F., et al., 2010. TBC1D1 regulates insulin- and contraction-induced glucose transport in mouse skeletal muscle. Diabetes 59(6): 1358–65, Doi: 10.2337/db09-1266.

[56] Chen, Q., Xie, B., Zhu, S., Rong, P., Sheng, Y., Ducommun, S., et al., 2017. A Tbc1d1Ser231Ala-knockin mutation partially impairs AICAR- but not exercise-induced muscle glucose uptake in mice. Diabetologia 60(2): 336–45, Doi: 10.1007/s00125-016-4151-9.

[57] Kjøbsted, R., Roll, J.L.W., Jørgensen, N.O., Birk, J.B., Foretz, M., Viollet, B., et al., 2019. AMPK and TBC1D1 regulate muscle glucose uptake after, but not during, exercise and contraction. Diabetes 68(7): 1427–40, Doi: 10.2337/db19-0050.

[58] Raun, S.H., Henriquez-Olguín, C., Karavaeva, I., Ali, M., Møller, L.L.V., Kot, W., et al., 2020. Housing temperature influences exercise training adaptations in mice. Nature Communications, Doi: 10.1038/s41467-020-15311-y.

[59] McKie, G.L., Medak, K.D., Knuth, C.M., Shamshoum, H., Townsend, L.K., Peppler, W.T., et al., 2019. Housing temperature affects the acute and chronic metabolic adaptations to exercise in mice. Journal of Physiology, Doi: 10.1113/JP278221.

[60] Lassiter, D.G., Sjögren, R.J.O., Gabriel, B.M., Krook, A., Zierath, J.R., 2018. AMPK activation negatively regulates GDAP1, which influences metabolic processes and circadian gene expression in skeletal muscle. Molecular Metabolism 16: 12–23, Doi: 10.1016/j.molmet.2018.07.004.

[61] Scheffler, T.L., Park, S., Roach, P.J., Gerrard, D.E., 2016. Gain of function AMP-activated protein kinase γ3 mutation (AMPKγ3R200Q) in pig muscle increases glycogen storage regardless of AMPK activation. Physiological Reports 4(11), Doi: 10.14814/phy2.12802.

[62] Skurat, A. V., Peng, H.L., Chang, H.Y., Cannon, J.F., Roach, P.J., 1996. Rate-determining steps in the

872 biosynthesis of glycogen in COS cells. Archives of Biochemistry and Biophysics 328(2): 283–8, Doi:
873 10.1006/abbi.1996.0174.

874

875

Figure legends:

Figure 1: Tamoxifen-induced deletion of AMPKα subunits in adult mice

A-F: Muscle-specific deletion of AMPKα1 and α2 was obtained by expressing a tamoxifen-inducible Cre-recombinase construct driven by the human skeletal muscle actin promotor. The tamoxifen treatment protocol consisted of three single injections (40 mg/kg bw) each separated by 48 hours and mice were investigated 1, 3 and 8 weeks after the last tamoxifen injection. For the vehicle experiment, all mice received injections containing sunflower oil. Gene-expression of AMPKα1 and α2 subunits was measured in EDL muscle. Protein levels of AMPKα1 and α2 were measured in EDL and heart from control and AMPKα imdKO mice. These data from the AMPKα imdKO model were compared to conventional AMPKα double KO model (AMPKα mdKO) with chronic lack of AMPK function. Protein levels were measured by immunoblotting and gene-expression was measured by real time PCR and presented relative to TATA-Box Binding Protein (TBP). Data have been normalized to control mice (=100%). Data are given as means ± SEM (n=5-6 within each group).
One-way ANOVA was used for comparing 1 wk, 3 wks and 8 wks to vehicle control within AMPKα imdKO mice. Additional t-test was applied for comparison of AMPKα imdKO with control mice within each given time point. * $p \leq 0.05$, ** $p \leq 0.01$ and *** $p \leq 0.001$ for difference from corresponding control mice. ## $p \leq 0.01$ and ### $p \leq 0.001$ for difference from corresponding AMPKα imdKO vehicle. ††† $p \leq 0.001$ for difference from 1 week AMPKα imdKO.

Figure 2: Normal insulin action despite acute deletion of catalytic AMPK function in skeletal muscle. A-B: 3 weeks after the last tamoxifen injection, control and AMPKα imdKO mice were fasted for 5 hours before they were given an intraperitoneal injection of glucose (2 g/kg body weight) dissolved in a 0.9% saline solution. Blood was sampled from the tail vein and analyzed for glucose concentration by a glucometer before (0 min) and 20, 40, 60, 90 and 120 min after injection. Plasma insulin levels were determined at 0, 20, and 40 min using an insulin ELISA assay (n=10-12). C: For the insulin tolerance test (ITT), mice were fasted for 2 hours and insulin was injected intraperitoneally (1 U/kg body weight, Actrapid, Novo Nordisk, Bagsværd, Denmark). Tail vein blood glucose concentration was measured before (0 min), 20, 40 and 60 min after injection (n=10-12). D-E: Isolated

EDL and soleus muscles from control and AMPKα imdKO mice were incubated for 30 min in the absence (basal) or presence of 100 µU/ml and 10,000 µU/ml insulin and muscle glucose uptake was determined by measuring the accumulation of intracellular [^{3}H]-2-deoxyglucose (2DG) (n=6-8). F-H: Key insulin signaling intermediates in EDL muscle from control and AMPKα imdKO mice were investigated by immunoblotting and are given as representative immunoblots.

Data are given as means ± SEM. Two-way RM ANOVA was used to investigate the effect of genotype and time (GTT and ITT) or genotype and insulin concentrations (2DG uptake). ### $p \leq 0.001$ for significantly different from basal (0 min). ** $p \leq 0.01$ and *** $p \leq 0.001$ for significantly different compared to basal. §§ $p \leq 0.01$ and §§§ $p \leq 0.001$ for significantly different from 100 µU/ml. Line indicates main effect.

Figure 3: Acute deletion of muscle AMPK impairs maximal running speed and reduces muscle glycogen content and UGP2 expression. A: Maximal running speed during an incremental running test on a treadmill was assessed in control and AMPKα imdKO mice 1 and 3 wks after last tamoxifen injection and compared to before tamoxifen treatment (pre) (n=10-20 within each group). B: Muscle glycogen content in quadriceps muscle (normalized to control mice) was measured 1, 3 and 8 weeks after tamoxifen-induced deletion of AMPKα and compared to vehicle control groups (n=5-6 within each group). C: 3 wks following last tamoxifen injection muscle glycogen in quadriceps muscle from control and AMPKα imdKO mice was measured in the rested state and following 30 min of treadmill exercise at the same relative intensity (n=8-13). D: Glycogen synthase activity was measured as fractional activity in the presence of 0.2 mM G6P and given relative to saturated conditions (8 mM G6P) (n=8-13). E: Protein levels of GLUT4, HKII, GP, GS and UGP2 in quadriceps muscle were measured by immunoblotting in control and AMPKα imdKO mice 3 wks following last tamoxifen injection (n=5-6). UGP2 mRNA content in quadriceps muscle was determined 1, 3 and 8 weeks after the last tamoxifen injection and compared to the vehicle group (sunflower oil) (n=5-6).

One-way ANOVA was used for comparing 1 wk, 3 wks and 8 wks to vehicle control within AMPKα imdKO mice. Additional t-test was applied for comparison of AMPKα imdKO with control mice within each given time point. The effect of exercise was investigated by a two-way ANOVA (C and D). Data are given as means ± SEM. * $p \leq 0.05$, ** $p \leq 0.01$ and *** $p \leq 0.001$ for effect of genotype

within a given time-point. ### p≤0.001 for difference from vehicle in AMPKα imdKO mice. §§ p≤0.01 for main effect of exercise. Line indicates main effect.

Figure 4: Regulation of myocellular nucleotide pool during exercise.

Overview of cellular processes regulating cellular nucleotide balance. The increasing ATP utilization during exercise leads to ATP regeneration through the adenylate kinase reaction (2 ADP→ AMP + ATP), which increases accumulation of AMP. In order to avoid a large accumulation of AMP in the cell, AMP is deaminated to IMP via the enzyme AMP deaminase (AMPD). Intracellular IMP, formed during exercise, can be degraded to inosine (INO) and hypoxanthine (HX), which can leave the muscle cell potentially causing a nucleotide loss. cN-II: Cytosolic nucleotidase II, cN-IA: Cytosolic nucleotidase IA, PNP: Purine nucleoside phosphorylase, P_i: Inorganic phosphate, NH_3: Ammonia.

Figure 5: AMPK is necessary to maintain the cellular nucleotide pool during exercise.

A-G: Control and AMPKα imdKO mice performed 30 min of treadmill exercise at the same relative intensity and were compared to corresponding resting mice. Concentration of adenosine triphosphate (ATP), adenosine diphosphate (ADP), adenosine monophosphate (AMP), inosine monophosphate (IMP), hypoxanthine (HX), adenosine (ADO) and inosine (INO) were measured in quadriceps muscle (n=6-8). H-I: AMPD activity and AMPD1 protein content was measured in quadriceps muscle (n=6-8). Data are given as means ± SEM. Two-way ANOVA was used for statistical analyses of genotype and exercise. ** p≤0.01 and *** p≤0.001 for significant effect of genotype. §§ p≤0.01 and §§§ p≤0.001 for difference from resting. Line indicates main effect.

Figure 6: AMPK is dispensable for regulation of muscle substrate utilization and mitochondrial function.

A: RER before, during and after 30 min of a single treadmill exercise bout at 60% of individual maximal running speed (n=18-20). B: Palmitate oxidation was measured *ex vivo* in resting or contracting soleus muscles from control and AMPKα imdKO mice (n=15-18). C. Protein levels of plasma membrane fatty acid binding protein (FABPpm) and cluster of differentiation (CD) 36 were

analyzed in TA muscle by immunoblotting (n=8-13). D: Mitochondrial respiration rates measured during cumulative addition of substrates in permeabilized TA fibers (n=9-12). Abbreviations: CI_P: Maximal complex I respiration, $CI+II_P$: Maximal complex I+II linked respiration (capacity for oxidative phosphorylation), ETS (CI+II): Electron transport system capacity (uncoupled respiration) through complex I and II, ETS (CII): Electron transport system capacity through complex II. E: Protein levels of mitochondrial subunits for complex I, II, III, IV and V in TA muscle were determined by immunoblotting (n=17-18). Data are given as means ± SEM. The effect of exercise and genotype was investigated by two-way ANOVA. §§§ $p \leq 0.001$ for difference from resting. Line indicates main effect.

Figure 7: AMPK is not required for exercise and contraction-stimulated glucose uptake in skeletal muscle.

A-C: Control and AMPKα imdKO mice were either rested or performed 30 min treadmill exercise at the same relative intensity. Phosphorylation of AMPKα Thr172, TBC1D1 Ser231 and ACC Ser212 was determined in quadriceps muscle by immunoblotting (n=8-13). D-E: Blood glucose concentration and muscle lactate concentration in quadriceps muscle was measured under resting conditions and following 30 min of treadmill exercise (n=8-13). F: Muscle glucose uptake during 30 min of treadmill exercise was measured in TA, soleus, EDL and quadriceps muscle from control and AMPKα imdKO mice (n=8-13). G-H: Isolated EDL and soleus muscle from control and AMPKα imdKO mice were electrically forced to contract and glucose uptake was measured in resting and contracting muscles (n=4-8). Data are given as means ± SEM. The effect of genotype and exercise/muscle contraction was investigated by two-way ANOVA. ** $p \leq 0.01$ and *** $p \leq 0.001$ for significant effect of genotype. § $p \leq 0.05$, §§ $p \leq 0.01$ and §§§ $p \leq 0.001$ for difference from resting. Line indicates main effects.

Tables:

Table 1: Body composition of control and AMPKα imdKO mice

	Pre tamoxifen treatment		3 wks post tamoxifen treatment			
	control	**imdKO**	**control**	**imdKO**	**Main effect**	**Interaction**
Weight (g)	26.3 ± 0.4	26.3 ± 0.5	25.7 ± 0.5	25.3 ± 0.4	***	-
Fat mass (g)	2.0 ± 0.2	1.8 ± 0.2	2.2 ± 0.1	2.1 ± 0.1	*	-
LBM (g)	21.9 ± 0.3	22.3 ± 0.4	21.8 ± 0.4	21.5 ± 0.3	-	p = 0.003

Body composition was investigated before (pre) and 3 weeks after (post) tamoxifen treatment. Data are given as means ± SEM (n=20). * $p < 0.05$ and *** $p < 0.001$ for significant difference from pre treatment independently of genotype.

Table 2: Tissue weight in control and AMPKα imdKO mice.

	Weight (mg)		
Tissue	**control**	**imdKO**	**p-value**
Tibialis anterior	42 ± 1	43 ± 1	0.49
Heart	101 ± 3	98 ± 3	0.52
WAT	200 ± 14	245 ± 37	0.28
Liver	991 ±79	988 ± 78	0.98
Kidney	134 ± 6	136 ± 10	0.90

Weight (mg) of tibialis anterior muscle, heart, white subcutaneous adipose tissue (WAT), liver, and kidney was investigated 3 weeks after (post) tamoxifen treatment. Data are given as means ± SEM (n=8-12).

Table 3: AMPD kinetic properties

	WT	imdKO	p-value
V_{max} (µmol • min^{-1} • g^{-1})	479 ± 47	541 ± 83	0.35
K_m (mM)	0.27 ± 0,05	0.37 ± 0,13	0.46

Kinetic properties for AMPD (V_{max} and K_m) in basal quadriceps muscle were analyzed in homogenate in the presence of 15 mM, 0.1 mM, 0.06 mM, and 0.04 mM AMP and the formation of IMP was quantified by HPLC. Data are given as means ± SEM (n=6-8).

1A

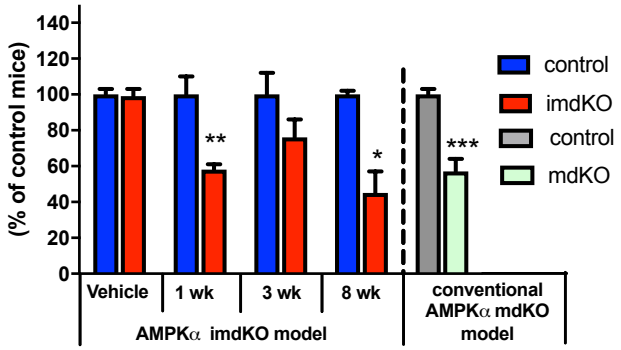

1B

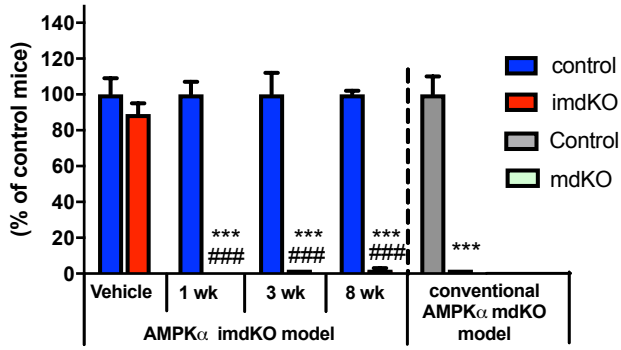

1C

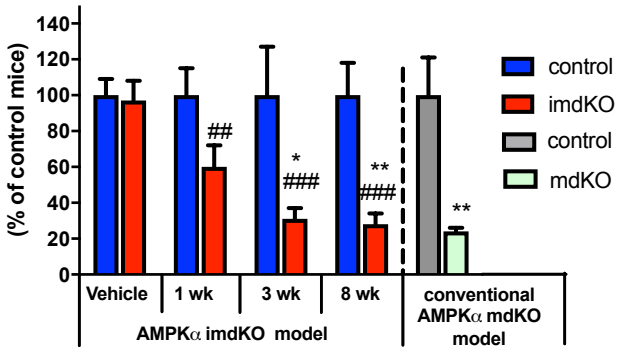

1D

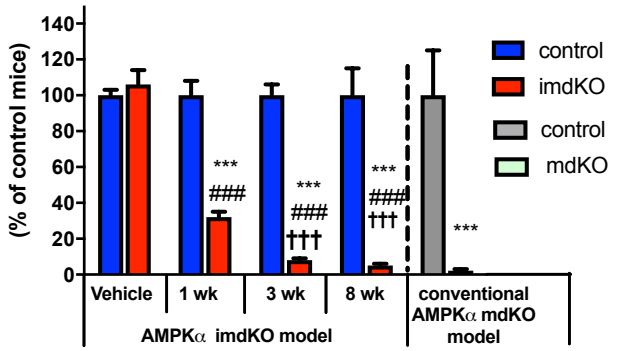

1E

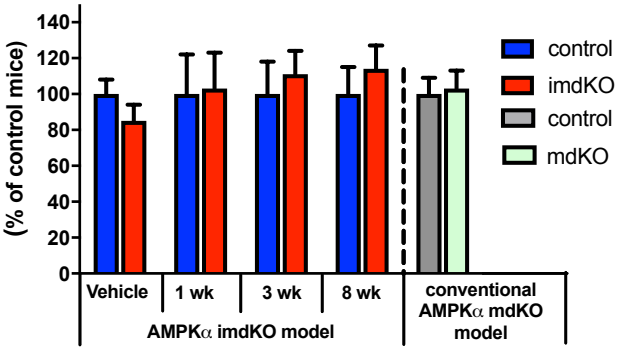

1F

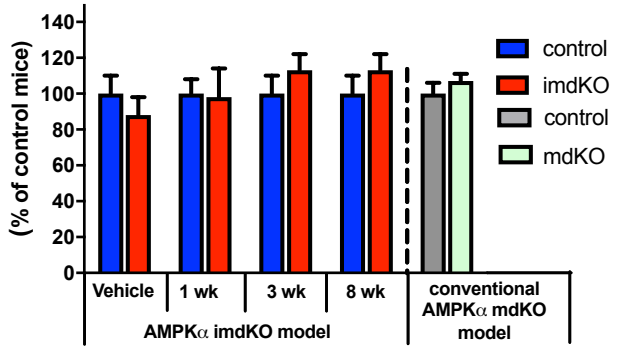

2A

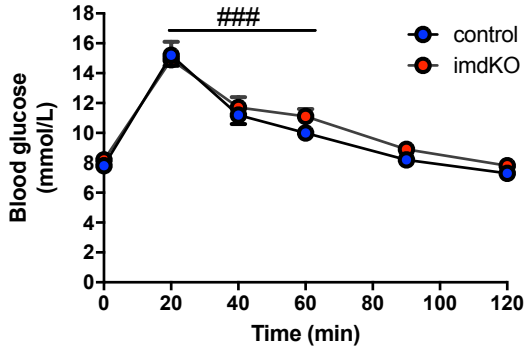

2B

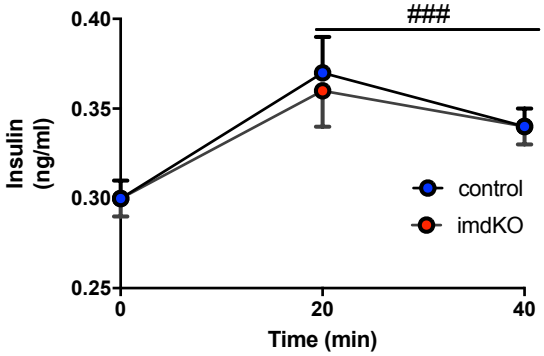

2C

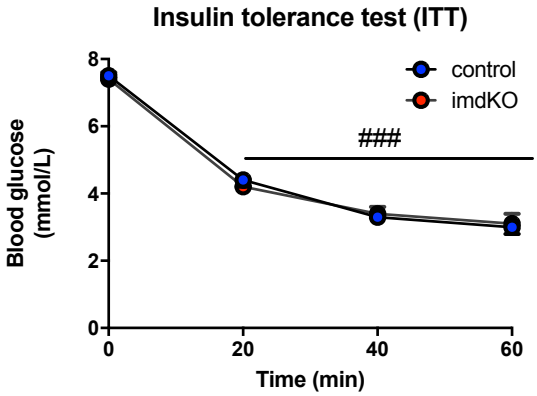

2D

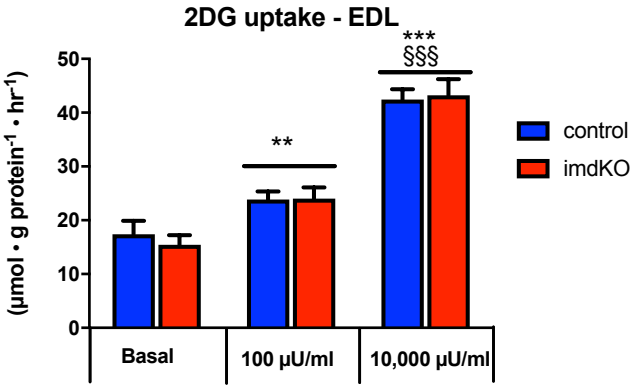

2E

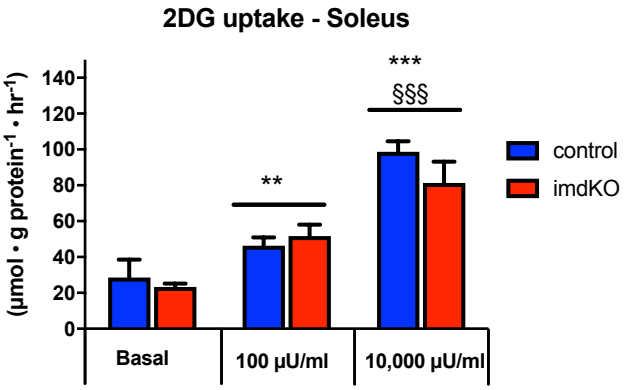

2F

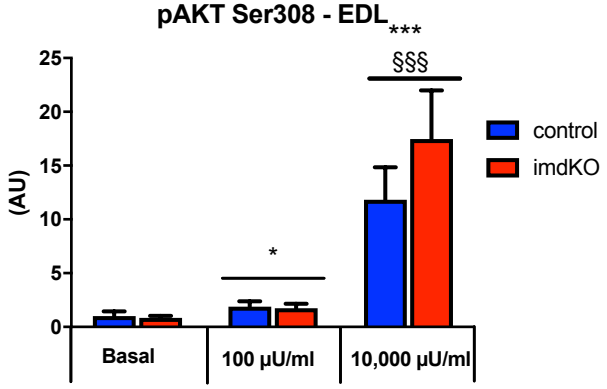

2G

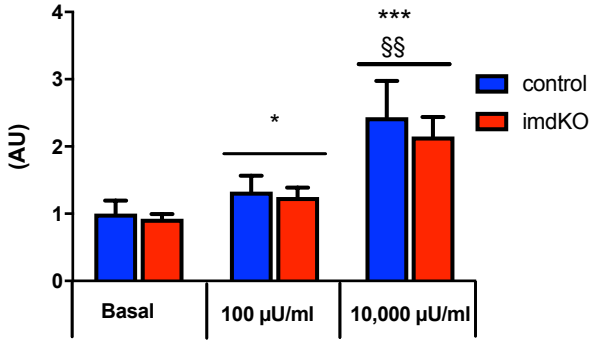

2H

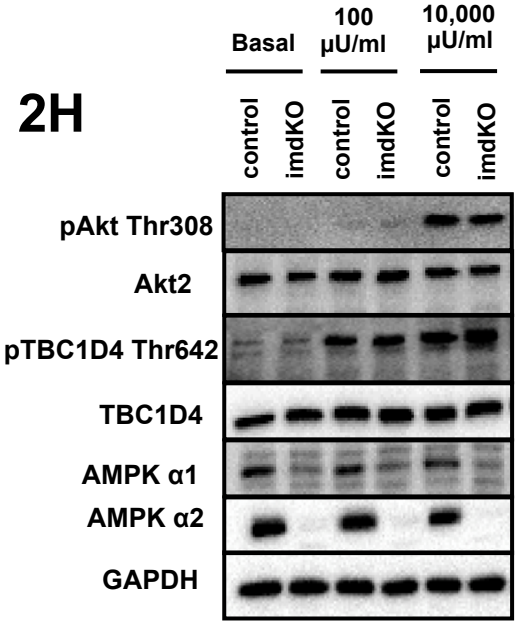

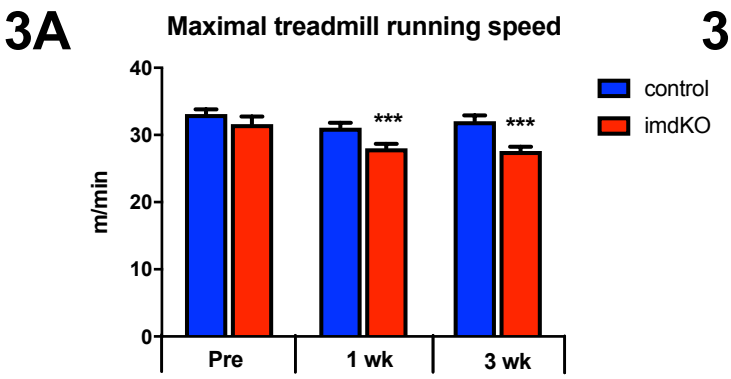
3A
Maximal treadmill running speed
m/min
40
30
20
10
0
***
***
Pre
1 wk
3 wk
control
imdKO

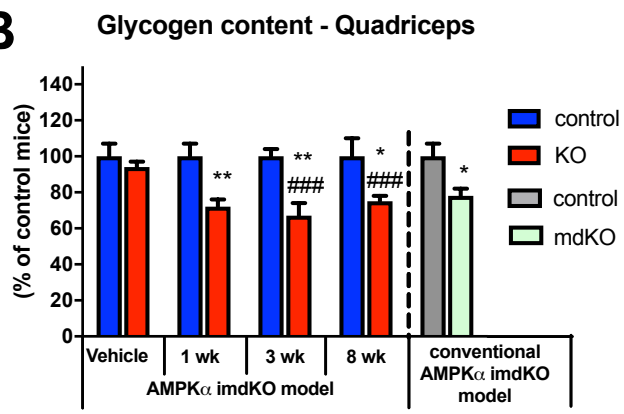
3B
Glycogen content - Quadriceps
(% of control mice)
140
120
100
80
60
40
20
0
**
**
###
*
###
*
Vehicle
1 wk
3 wk
8 wk
AMPKα imdKO model
conventional AMPKα imdKO model
control
KO
control
mdKO

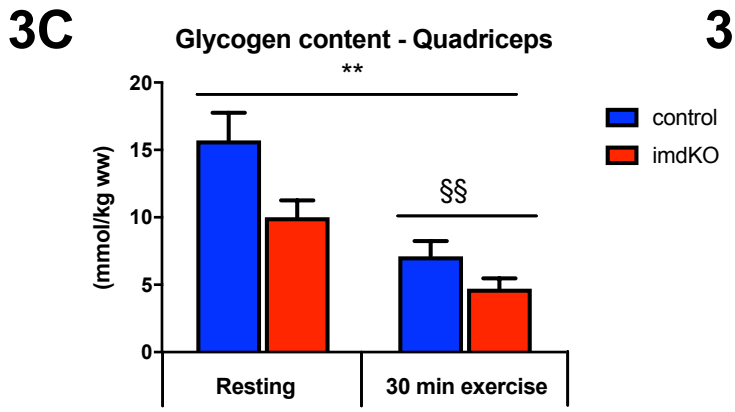
3C
Glycogen content - Quadriceps
(mmol/kg ww)
20
15
10
5
0
**
§§
Resting
30 min exercise
control
imdKO

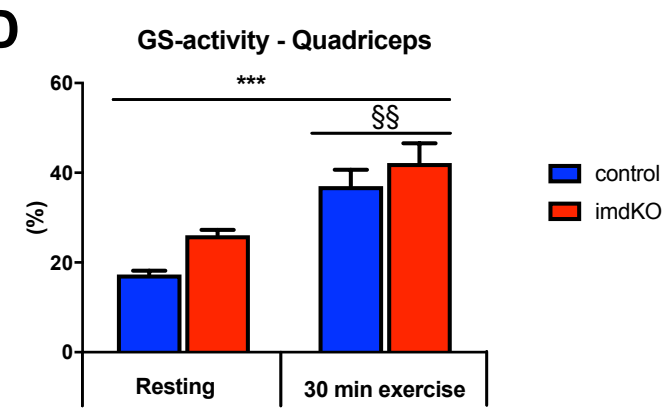
3D
GS-activity - Quadriceps
(%)
60
40
20
0
***
§§
Resting
30 min exercise
control
imdKO

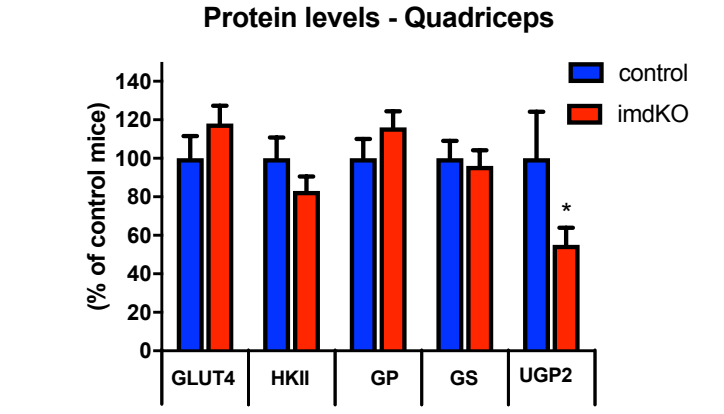
3E
Protein levels - Quadriceps
(% of control mice)
140
120
100
80
60
40
20
0
*
GLUT4
HKII
GP
GS
UGP2
control
imdKO

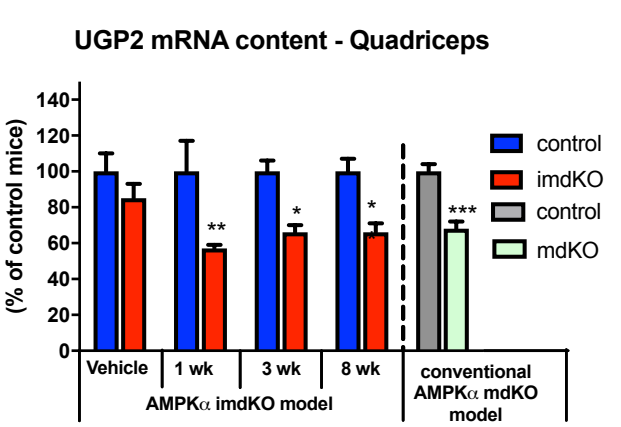
3F
UGP2 mRNA content - Quadriceps
(% of control mice)
140
120
100
80
60
40
20
0
**
*
*
***
Vehicle
1 wk
3 wk
8 wk
AMPKα imdKO model
conventional AMPKα mdKO model
control
imdKO
control
mdKO

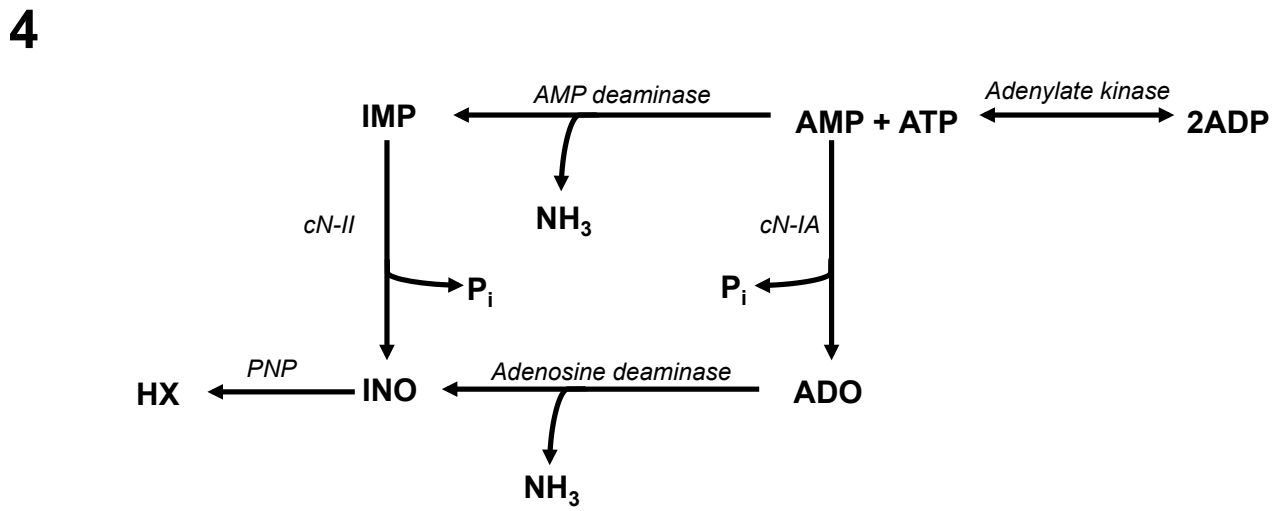
4
IMP
AMP deaminase
NH3
AMP + ATP
Adenylate kinase
2ADP
cN-II
Pi
cN-IA
Pi
HX
PNP
INO
Adenosine deaminase
ADO
NH3

5A

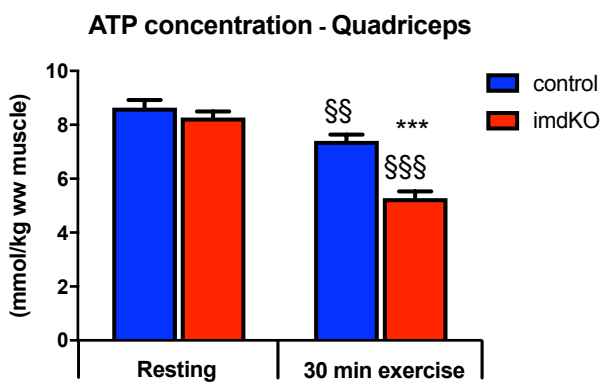

5B

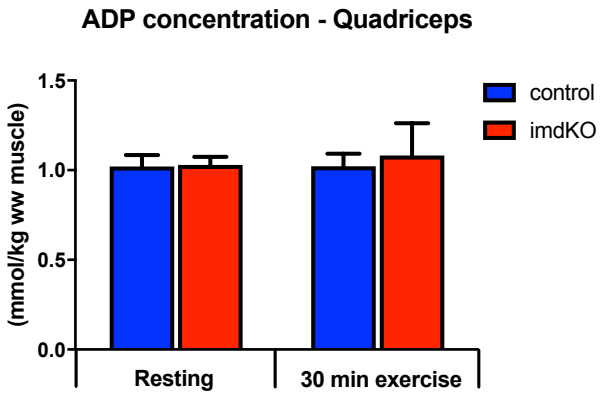

5C

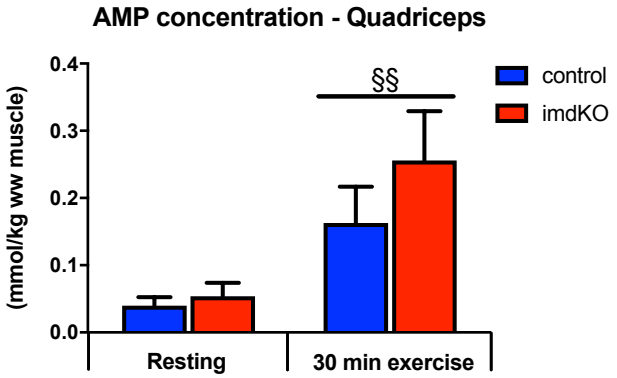

5D

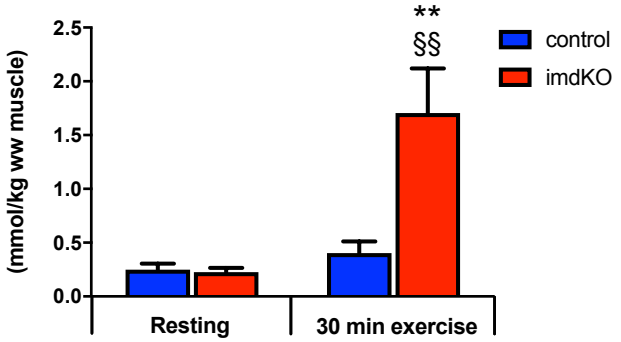

5E

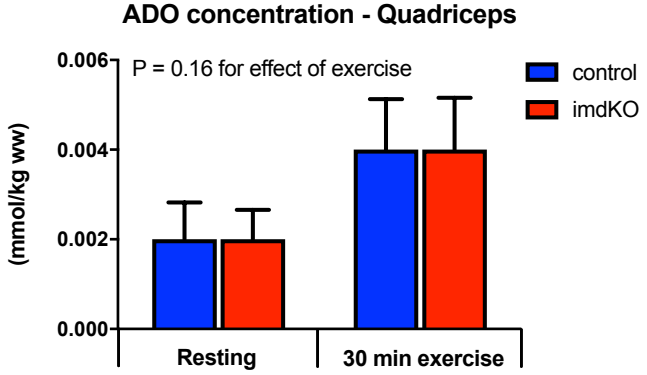

5F

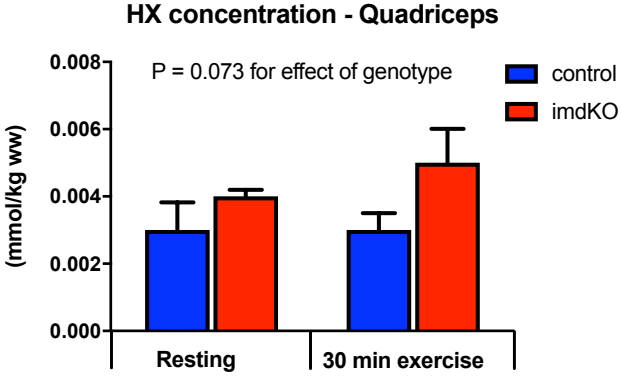

5G

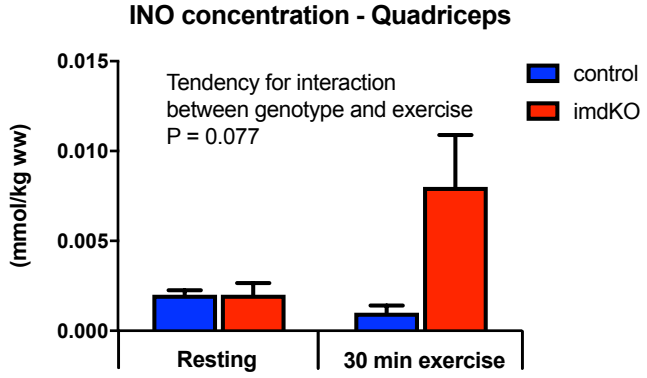

5H

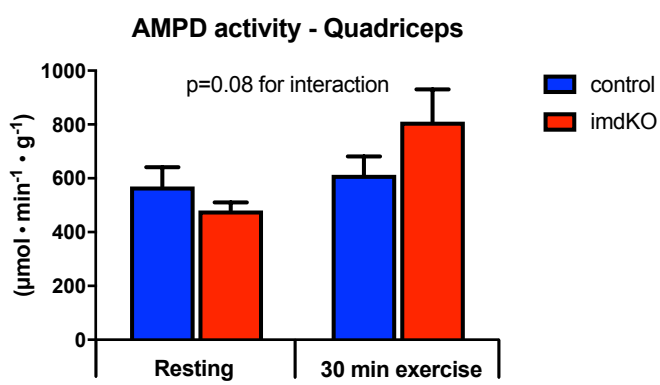

5I

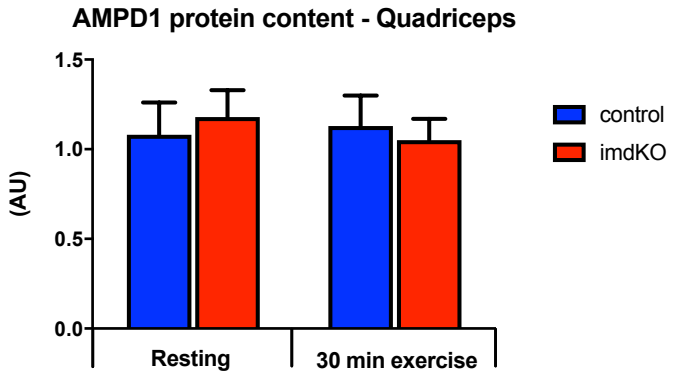
AMPD1 protein content - Quadriceps
1.5
1.0
0.5
0.0
(AU)
Resting
30 min exercise
control
imdKO

6A

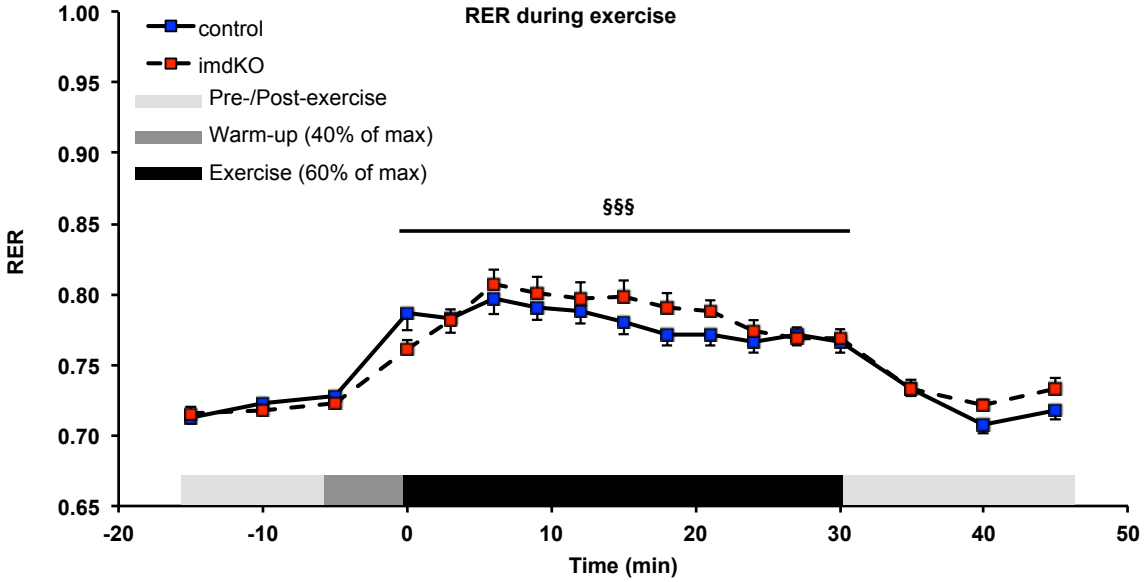
RER during exercise
control
imdKO
Pre-/Post-exercise
Warm-up (40% of max)
Exercise (60% of max)
§§§
RER
1.00
0.95
0.90
0.85
0.80
0.75
0.70
0.65
-20
-10
0
10
20
30
40
50
Time (min)

6B

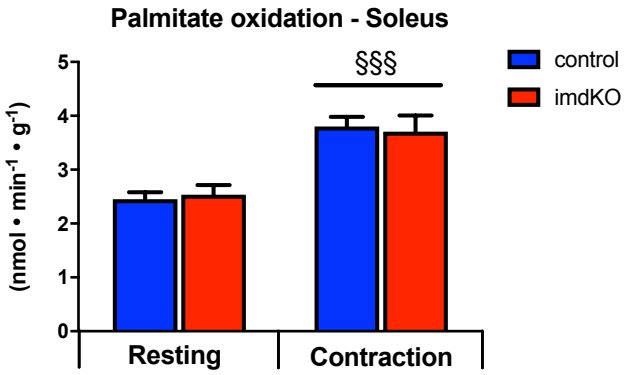
Palmitate oxidation - Soleus
§§§
control
imdKO
(nmol • min-1 • g-1)
5
4
3
2
1
0
Resting
Contraction

6C

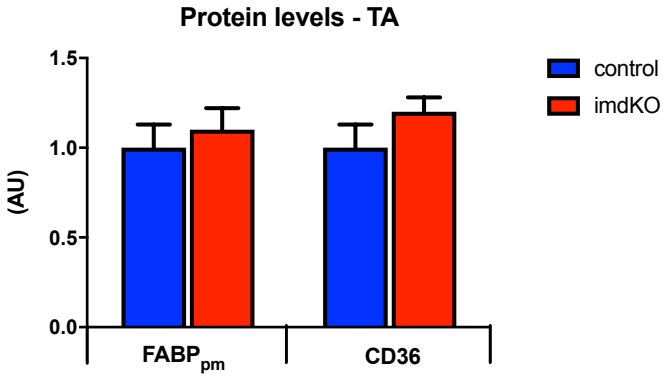
Protein levels - TA
control
imdKO
(AU)
1.5
1.0
0.5
0.0
FABPpm
CD36

6D

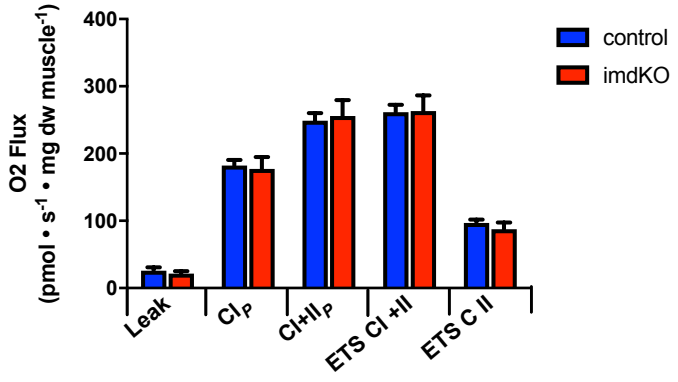
Mitochondrial respiration - TA
control
imdKO
O2 Flux
(pmol • s-1 • mg dw muscle-1)
400
300
200
100
0
Leak
CIp
CI+IIp
ETS CI +II
ETS C II

6E

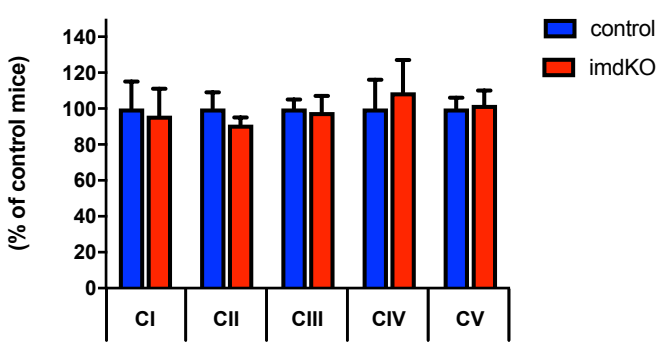
Mitochondrial protein levels - TA
control
imdKO
(% of control mice)
140
120
100
80
60
40
20
0
CI
CII
CIII
CIV
CV

7A

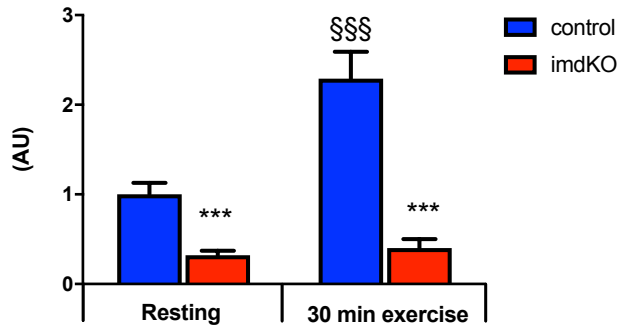

7B

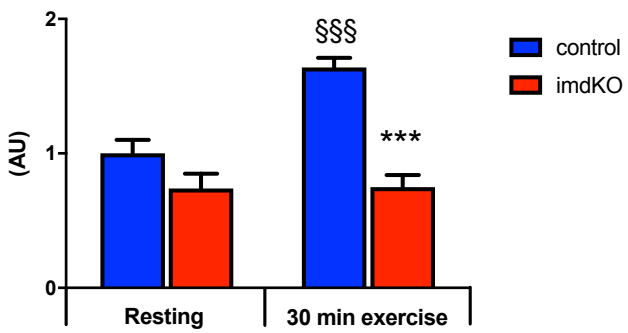

7C

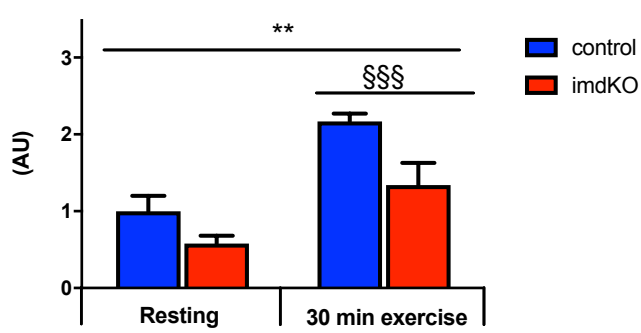

7D

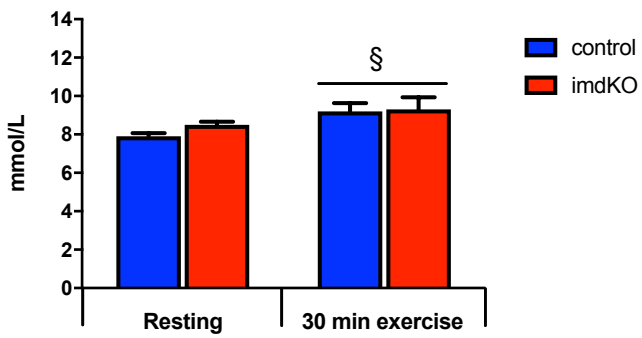

7E

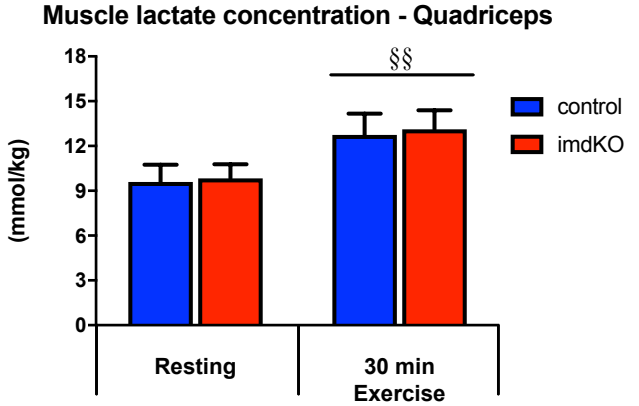

7F

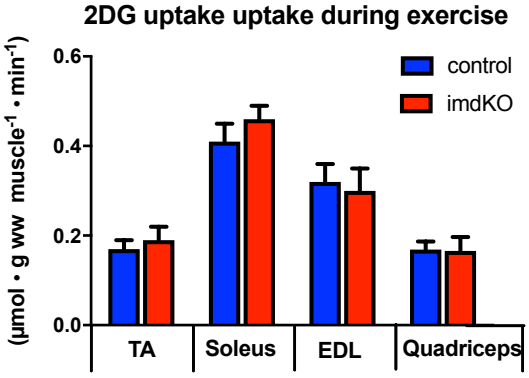

7G

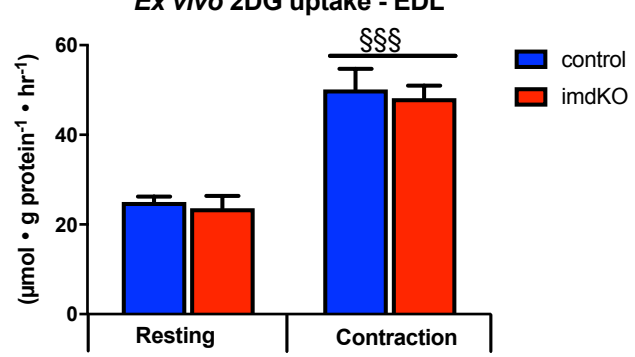

7H